AIMS Energy, 14(1): 47–88.
DOI: 10.3934/energy.2026003
Received: 20 June 2025
Revised: 29 October 2025
Accepted: 25 November 2025
Published: 07 January 2026

https://www.aimspress.com/journal/energy

Research article

Advanced optimization for sustainable energy management: A case study of microgrid design in Niamey, Niger using the transient search algorithm

Issoufou Tahirou Halidou[1,*], M.H. Elkholy[2], Akie Uehara[1], Fathia Jombi Kheir[1], Mitsunaga Kinjo[1], Tomonobu Senjyu[1], M. Talaat[3,4], Abdoulkader Moussa Siddo[5] and Taghreed Said[6]

[1] Faculty of Engineering, University of the Ryukyus, Okinawa 903-0213, Japan
[2] Interdisciplinary Research Center for Smart Mobility and Logistics, King Fahd University of Petroleum and Minerals, Dhahran 31261, Saudi Arabia
[3] Electrical Power and Machines, Faculty of Engineering, Zagazig University, P.O. 44519, Zagazig, Egypt
[4] Faculty of Engineering and Technology, Egyptian Chinese University, P.O. 11787, Cairo, Egypt
[5] Division of Civil and Environmental Engineering, Kitami Institute of Technology, Kitami, Hokkaido 090-8507, Japan
[6] Electrical Engineering and Computers Department, Higher Technological Institute, 10th of Ramadan City, Egypt

* **Correspondence:** Email: thissoufou@gmail.com; Tel: +22798459093.

Graphical abstract

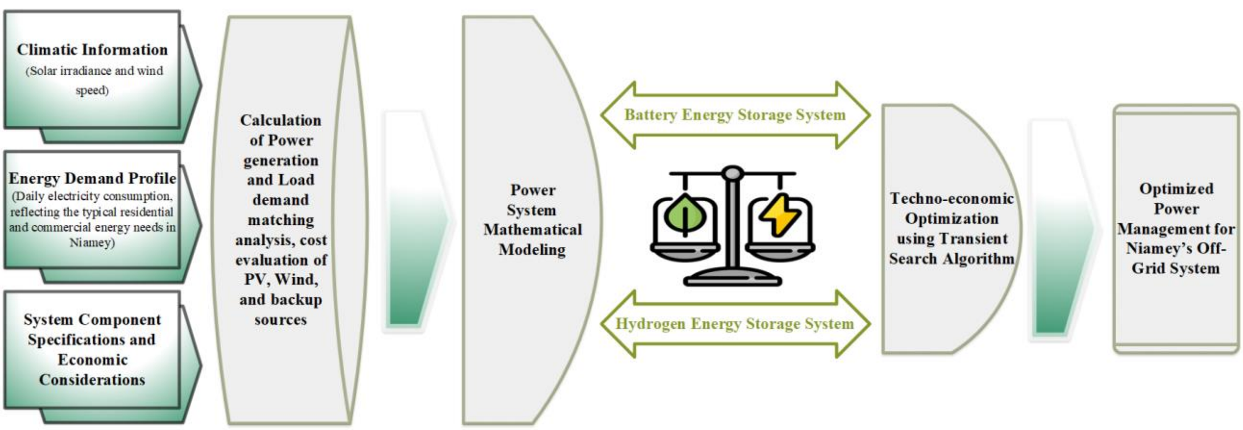

Abstract: In this study, we evaluated three renewable-based microgrid configurations designed to strengthen energy security and long-term sustainability. Configuration 1 integrates a photovoltaic (PV) array and wind turbines (WT) with a battery energy storage system (BESS). Configuration 2 replaces BESS with a hydrogen energy storage system (HESS), offering extended storage capacity and improved energy availability. Configuration 3 combines BESS and HESS, leveraging the advantages of short-term and long-term storage to create a more resilient energy system. The objective function was formulated to minimize the total annual cost (TAC) while optimizing energy generation, storage efficiency, and overall system reliability. A robust and efficient transient search algorithm (TSA) was employed to determine the optimal capacity of the microgrid configurations. A comprehensive cost analysis revealed that configuration 1 was the most cost-effective. However, incorporating HESS in configuration 2 resulted in a 41.3% increase in cost due to the investment required for electrolyzers, storage tanks, and fuel cells. Configuration 3, which integrates battery and hydrogen storage, incurred an additional 3.2% cost compared to configuration 2 and 45.8% compared to configuration 1. Despite the higher cost, this hybrid system enhances energy resilience by efficiently balancing short-term and long-term storage solutions.

Keywords: sustainable electricity supply; hybrid energy storage optimization; energy security in off-grid regions; transient search algorithm (TSA); resilient energy in Niamey

1. Introduction

1.1. General overview

Energy is essential for the growth of major and small-to-medium economies worldwide. Despite its vital significance to society, there have been persistent disagreements and varying viewpoints over the methods of energy generation. Conventional electricity generation methods have historically caused significant environmental damage, hence intensifying the critical issue of global warming [1–3]. As a result, sustainable technological advancements and environmentally friendly energy generation methods have been introduced and implemented in recent years to significantly reduce adverse environmental effects [4]. These are referred to here as renewable energy sources (RESs). RESs are pervasive and abundant [5]. They generate low-cost, sustainable, and clean electricity [6]. They are infinite, long-lasting energy sources available worldwide. Several energy sources, such as PV systems and WT have emerged as attractive alternatives [7]. Thanks to their cost-effectiveness, abundance, and low or zero carbon emissions, they have been deployed worldwide in suitable regions [8]. A key drawback of renewable sources mentioned earlier is their inherent intermittency, which is significantly influenced by weather circumstances and the time of day [9]. These factors result in changes in energy output and severely impact the reliability and consistency of power systems, highlighting the urgency of addressing this issue. Implementing hybrid renewable energy systems (HRES) solutions becomes a viable solution to this pressing issue [10]. The integration of storage systems improves the reliability and stability of renewable energy-based systems, ensuring a more consistent power supply even during periods of reduced renewable energy generation [11].

1.2. Literature review

Substantial advancements have been made in forging hybrid PV and wind energy systems for remote locations [12]. Many researchers have investigated microgrid systems operating autonomously to supply electricity to isolated communities without access to a reliable utility grid [13]. A microgrid is an autonomous power system with diverse distributed energy sources, storage systems, and integrated loads. It can operate autonomously or be integrated with the main grid to provide cost-effective, reliable, and clean electricity [14]. Renewable energy combined with storage technologies creates new opportunities for electricity consumers to achieve independence from the grid or any particular import power and fulfill their energy requirements autonomously [15]. Furthermore, the increasing incorporation of RESs into power generation systems necessitate the significant contribution of energy storage systems (ESSs) in improving power quality, reliability, and sustainability, thereby enhancing system efficiency and offering the further integration of RESs. The main purpose of ESSs in renewable energy systems is to thoroughly compensate for the supply-demand mismatch when renewable sources cannot satisfy the load demands [16]. In Ref. [17], a metaheuristic approach was employed to optimize the size of the ESSs based on batteries in hybrid power systems. The researchers in Ref. [18] incorporated particle swarm optimization (PSO) with constraint techniques to reduce the overall costs, netload, and carbon dioxide (CO_2) emissions of an independent hybrid system employing PV, diesel, and battery power to meet the energy demands of 20 households. The researchers in Ref. [19] compared battery and hydrogen storage within a grid-connected PV system in Sweden. Their findings indicated that hydrogen storage performs inferior to battery storage in terms of net present value (NPV) and self-sufficiency ratio. In Ref. [20], mixed integer linear programming (MILP), in combination with the hybrid optimization of multiple energy resources (HOMER) and general algebraic modeling system (GAMS), was used to model and optimize a standalone microgrid using a hybrid PV and wind energy system and a BESS. Using demand response (DR) in the system reduced battery and inverter capacities by 35.6% and 35%, reducing overall system costs by 17.1% and increasing load factor by 57.9%, improving system reliability and performance. Ref. [21] considered the annual cost and CO_2 emissions as objectives in scaling and designing solar PV systems, fuel cells (FCs), and BESS. The researchers in Ref. [22] investigated the techno-economic performances of a highly renewable energy-based standalone microgrid comprised of PV, WT, and diesel generator (DG), with either BESS or pumped thermal energy storage (PTES), considering demand-side management strategies for different system design scenarios. The results indicate that, compared to using BESS, the PV-WT-PTES configuration emerged as the most efficient in terms of technology and economics for the microgrid under examination. In Ref. [23], a micro-pumped hydro energy storage (PHES) system and BESS were integrated into small-scale renewable energy systems and compared to assess efficiency, cost, maturity, and storage duration for a remote area in Sweden. The PV-WT-BESS has demonstrated its superiority over the PV-WT-micro PHES system in terms of economic benefits and reliability, resulting in an 18.61% lower life cycle cost (LCC) and 6.12% less oversupply. In Ref. [24], a stochastic techno-economic comparison was conducted using microgrid modeling and Monte Carlo techniques to compare long-duration flywheels (LD FES), lithium-ion batteries (Li-ion BESS), and lead-acid batteries (Pb-Acid BESS) for off-grid and industrial facilities. The results have shown that incorporating LD FES in isolated microgrids and industrial facilities will yield a 39.6% and 34.1% chance, respectively, of generating a lower levelized cost of electricity (LCOE) and a 56.7% and 60.5% chance, respectively, of creating a lower levelized cost of storage compared to off-grid and industrial facilities with Li-ion BESS and Pb-Acid BESS. The researchers in Ref. [25] investigated the techno-economic aspects of an off-grid PV/biomass hybrid system, comparing three battery technologies using flower pollination harmony search (FPHS), artificial bee colony (ABC), and firefly algorithms. The findings demonstrated that the firefly algorithm performed the optimal configuration with the most inferior net present cost (NPC), highlighting the significance of selecting the suitable optimization technique. The HOMER software was utilized to investigate the techno-economic performance of a solar PV/DG hybrid system incorporating energy storage options, including lead-acid batteries, lithium-ion batteries, vanadium redox batteries, and zinc-bromine flow batteries, for the isolated Andaman & Nicobar and Lakshadweep islands of India [26]. Solar PV/DG/zinc-bromine flow hybrid system emerged as the most techno-economically viable optimized solution for both locations with the best system cost, the highest value of return of investment, renewable penetration and energy produced, and lowest pollutant emission and simple payback period. The researchers in Ref. [27] studied the techno-economic feasibility of solar-based hybrid plants with BESS-PTES under current and future cost reduction scenarios. The results indicated that BESS-PTES was more cost-effective than single energy storage for meeting high-reliability requirements. The researchers in Ref. [28] employed the BESS-supercapacitor (SC) technology to minimize the unused wind power in off-grid wind power systems. They developed a model that considers annual profit and wind curtailment, and they used a non-dominated sorting genetic algorithm (NSGA-II) and decision-making method to find the best configuration for the HRES.

1.3. Motivation and research gaps

Despite significant energy resources such as uranium (the world's seventh-largest producer [29]), mineral coal, natural gas, abundant sunlight, and the Niger River, Niger continues to rely heavily on electricity imports from Nigeria. Since the 1977 agreement, almost 75% of the national electricity demand has been met through this deal.

Nigeria hosts one of the largest dams in the region, the Kainji Dam, on the Niger River. Niger embarked on constructing its hydropower plant, the Kandadji Dam, triggering concerns from Nigeria about potential downstream water scarcity. Due to these concerns, Niger had to either abandon or suspend the Kandadji Dam project and negotiate with Nigeria for continued electricity supply. However, this significant reliance is fraught with risk as regular power outages continue.

In July 2023, political issues increased, resulting in the suspension of electricity exports from Nigeria to Niger and causing extensive power outages. This disruption significantly impacted daily life, key services, and economic activities, causing the nation to rely on diesel generators as the only alternative. This change posed considerable obstacles, such as increased operational costs and adverse ecological effects, further highlighting the vulnerability of Niger's energy security. Unreliable electricity supply hampers the socio-economic development of Niger. Hospitals, schools, businesses, and households struggle to function effectively, underlining the critical need for a reliable, affordable, clean, and sustainable energy solution. To tackle these difficulties, there is an urgent need for cost-effective, sustainable, and resilient energy systems tailored to Niger's local context. This requires strengthening the nation's electricity generation and supply infrastructure by investigating diverse technological solutions to expand energy sources and maintain stability within the energy sector. Harnessing Niger's abundant renewable energy resources and expediting their implementation are crucial to meeting the rising energy demand driven by population growth and economic expansion.

Utilizing advanced optimization methods, like the TSA, to design and manage renewable energy-based microgrids presents a viable approach that can reduce import dependence, improve energy resilience, and promote sustainable development.

Niamey, the capital and largest city of Niger serving as the country's political, administrative, and cosmopolitan hub, has been selected as the study area.

In this study, we examined the design of a renewable energy-based microgrid to supply electricity to Niamey City and its surrounding areas. This approach could serve as an alternative to electricity imports from Birnin Kebbi (Nigeria) while representing a strategic step toward energy independence and enhanced resilience against external disruptions.

Our objective is to design a microgrid capable of addressing power shortages caused by the unavailability of imported electricity. The major energy sources are PV and WT. Incorporating backup power systems into the microgrid design is essential to maintaining electricity availability during prolonged periods of low renewable energy generation or unforeseen disruptions.

Despite the vital role of power imports in Niamey's energy sector, there exists a substantial gap in research about measures to alleviate the risks related to this reliance. Researchers primarily focuses on integrating renewable energy but often overlooks the vulnerabilities arising from Niamey's political and economic dependence on external power sources. This situation underlines the necessity for targeted research, considering the distinct external elements affecting Niamey's electrical supply. There is a critical research gap in developing hybrid systems that integrate solar PV, wind, battery storage, and hydrogen storage, particularly for regions like Niamey, which boast high solar potential yet experience frequent power supply disruptions.

Implementing hybrid energy systems in Niamey is often overlooked, despite the region's unique climatic, economic, and political conditions, which present challenges and opportunities for innovative energy solutions.

A comprehensive economic assessment comparing different hybrid microgrid configurations is lacking, particularly those that balance cost-effectiveness with environmental sustainability in Niamey. Researchers often neglect to evaluate NPC, LPSP, and environmental impacts relevant to Niamey, which are crucial for making informed decisions on energy infrastructure investments. This gap underscores the need for detailed economic evaluations tailored to Niamey to effectively inform policy-making and investment strategies. Furthermore, prior studies have predominantly emphasized the usual operating conditions of microgrids to ascertain the optimal sizing of the ESSs and subsequently assessed their efficacy in sustaining power supply during emergencies. In such cases, the sizing of ESSs is predominantly influenced by the initial design parameters, which can affect their capability to supply power during fault conditions. In conventional power systems, generation capacity is designed to effectively satisfy demand, as coal and gas generators are controlled. Nonetheless, renewable energy output is erratic in autonomous microgrids, and energy storage is costly. Trying for 0% load-shedding can substantially increase investment expenses. Consequently, it is imperative to balance cost and risk. Decision-makers can address this by establishing a risk threshold, enabling the microgrid to fulfill demand under typical conditions, except in extreme situations such as extended durations of low renewable energy production caused by adverse weather. Moreover, research frequently needs comprehensive techno-economic assessments of hybrid renewable energy systems explicitly suited to Niamey's unique socio-economic and environmental contexts. Additionally, more extensive case studies are required to examine the feasibility and effectiveness of hybrid renewable energy solutions in Niamey's political and infrastructural framework.

Although several researchers have examined hybrid renewable systems incorporating battery and hydrogen storage, most have been developed under general conditions or in different politico-geographical contexts. Few investigations have considered the specific realities of Niger, where persistent heat, frequent power import disruptions, and limited grid flexibility create distinct technical and economic challenges. In contrast, we focus on Niamey's local context and proposes a hybrid PV-WT-BESS-HESS system optimized for both reliability and cost-effectiveness under these severe conditions. The application of TSA provides an additional contribution, as this relatively new metaheuristic approach has rarely been used for hybrid energy storage optimization. By combining site-specific constraints, a novel optimization framework, and a long-term techno-economic assessment, this work extends the literature. It offers valuable insights into designing resilient microgrids for regions facing similar climatic and political vulnerabilities.

1.4. Paper contributions

Research into optimal ESSs sizing and operational methods is strategically required to improve the resilience and reliability of microgrid systems. This is especially crucial given Niamey's frequent supply outages and the growing demand for reliable energy solutions. This study fills critical understanding and implementation gaps for hybrid renewable energy solutions in Niamey's grid-connected systems. Overall, the key contributions of this paper are as follows:

1. We present an innovative hybrid microgrid design that integrates solar PV systems, WT, BESS, and HESS, adapted to Niamey's particular climatic, economic, and political circumstances. This robust strategy effectively mitigates the vulnerabilities stemming from Niamey's reliance on energy imports from Nigeria, which were recurrently interrupted, particularly the significant supply line disruption observed from July 2023 to February 2024, owing to political complications. The study offers a secure and sustainable energy solution, alleviating the effects of political disruptions on Niamey's power supply.
2. We conduct a comprehensive techno-economic analysis of HRES designed for Niamey. It comprehensively evaluates this system's economic feasibility and sustainability by analyzing annual cost and environmental effects. This thorough method enables the assessment of the financial viability and enduring advantages of incorporating RESs in Niamey, hence promoting informed decision-making regarding energy investments.
3. We include extensive case studies of HRES initiatives that could be implemented in Niamey. These case studies look at the regulatory structures and socio-economic implications, providing valuable insights into the practical obstacles and potential of adopting hybrid systems in similar settings. This analysis contributes to the identification of optimal methods and the development of strategies for overcoming implementation challenges.
4. We identify the optimal configurations of HRES by analyzing residential consumption patterns and the renewable energy potential in Niamey. Additionally, we evaluate system efficiency using indicators such as annual cost and reliability. These indicators provide innovative perspectives on the trade-offs between initial investments, operational expenses, and environmental effects pertinent to Niamey. This thorough research verifies that the suggested configurations are both technically feasible and economically viable, offering a balanced approach to addressing Niamey's energy requirements, especially following interruptions in electricity supplies from a neighboring nation.

5. The proposed microgrid configuration and optimization strategy offer a scalable and adaptable model applicable to other African regions facing similar energy challenges. This novel approach facilitates the broader adoption of renewable energy and hybrid systems in developing countries with abundant solar potential and frequent power supply disruptions, enhancing energy resilience and stability.
6. The study underscores the importance of reliability and resilience in microgrid systems by introducing innovative approaches for optimizing ESSs sizing and operational planning. It defines risk thresholds and optimizes the balance between cost and risk to ensure an uninterrupted power supply, even in extreme scenarios such as minimal renewable generation or extended periods of adverse weather. This is especially crucial for Niamey, where the sudden shift in power in July 2023 underscored the necessity for a reliable and robust electricity supply.
7. We present innovative perspectives on policy and financial decisions by delivering specific recommendations informed by Niamey's specific economic, climatic, and political contexts. These insights inform the development of incentive schemes and financial models that can facilitate the adoption of renewable energy solutions, fostering a more self-sufficient and robust energy infrastructure in Niamey.

In addition to the above, we make a distinctive contribution by applying the TSA technique to optimize a hybrid PV-WT-BESS-HESS microgrid specifically designed for Niamey's operating environment. Unlike previous optimization approaches, TSA captures both the transient dynamics and stability features of complex systems, enabling a more balanced trade-off among cost, performance, and reliability. The model integrates Niamey's actual climatic data, socio-economic constraints, and risk factors related to power import interruptions. Through this integration, the study offers a clear and practical analysis of long-term energy resilience and sustainability. The results not only demonstrate the feasibility of the proposed configuration but also provide a decision-support framework for policymakers aiming to enhance energy autonomy and reduce vulnerability to external supply disruptions.

1.5. Paper organization

This paper is structured into 6 sections. In Section 2, "Materials and Methods", we provide an overview of the microgrid configuration, site-specific characteristics, and outlines microgrid mathematical modeling. In Section 3, "Illustration of the Proposed Hybrid System", we describe the three configurations and explain the coordination control of BESS and HESS. Section 4, "Problem Formulation and Proposed Optimization Algorithm," highlights the objective function and design constraints, describes the transient search algorithm and the verification of the proposed optimization algorithm. In Section 5, "Results and Discussions,", we discuss the case study, the findings of the three configurations, the system scalability and future adaptability, quantitative environmental impact and CO_2 reduction analysis, and the operational challenges and mitigation strategies. Section 6, "Conclusions," highlights the key contributions of this study.

2. Materials and methods

2.1. Overview of the microgrid configuration

Figure 1 depicts a schematic diagram of the proposed microgrid PV-WT power system with two

ESSs. The two energy storage alternatives (BESS/HESS) provide a reliable and sustainable power supply for the connected loads. The microgrid system utilizing an AC-coupled architecture is supposed to supply power for Niamey loads in case of any eventual interruption of the imported supply line from Birnin Kebbi (Nigeria), with photovoltaic and wind components as primary energy sources. ESSs technologies are employed to balance the supply-demand mismatch. The battery bank can be directly connected to the AC bus via a bi-directional converter, the HESS via a rectifier, and an inverter. We examine three system configuration scenarios: PV/WT/BESS constitutes Scenario 1, PV/WT/HESS Scenario 2, and PV/WT/BESS/HESS form the microgrid in Scenario 3. The load requirement is directly supplied from the primary power sources (PV and WT) for all three scenarios. The storage systems (BESS and HESS) help store excess energy produced during periods of high renewable generation and ensure a stable supply when renewable power is inadequate.

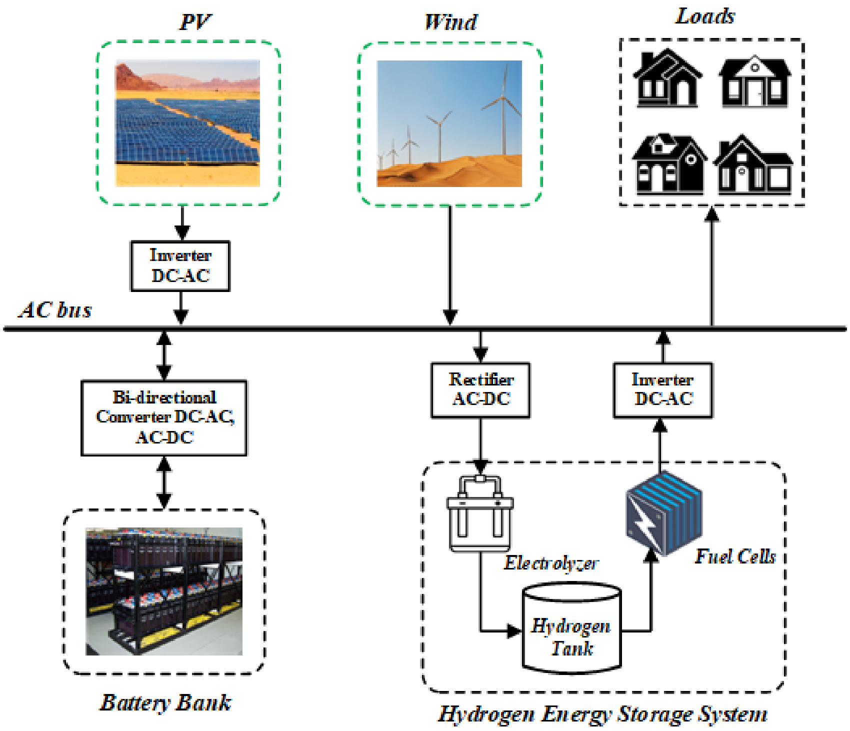

Figure 1. The topology of microgrid PV-Wind power system with BESS and HESS.

2.2. Site specific characteristics

With a land area of approximately 1,267,000 square kilometers, the Republic of Niger is the largest country in West Africa and the sixth largest in Africa. It shares borders in West Africa with seven countries: Algeria and Libya to the north, Benin and Nigeria to the south, Burkina Faso and Mali to the west, and Chad to the east. The desert covers over three-fourths of its land area in the north, where the highest temperatures on the earth's surface are recorded. The climate predominantly ranges from arid (Sahara Desert) in the north to semi-arid (Sahelian) in the central and southern regions. Niger's geographic location indicates that it is well-positioned to benefit from RESs, such as solar and wind energy, which are abundant and easy to use. Figure 2 illustrates the global horizontal solar radiation for Niger.

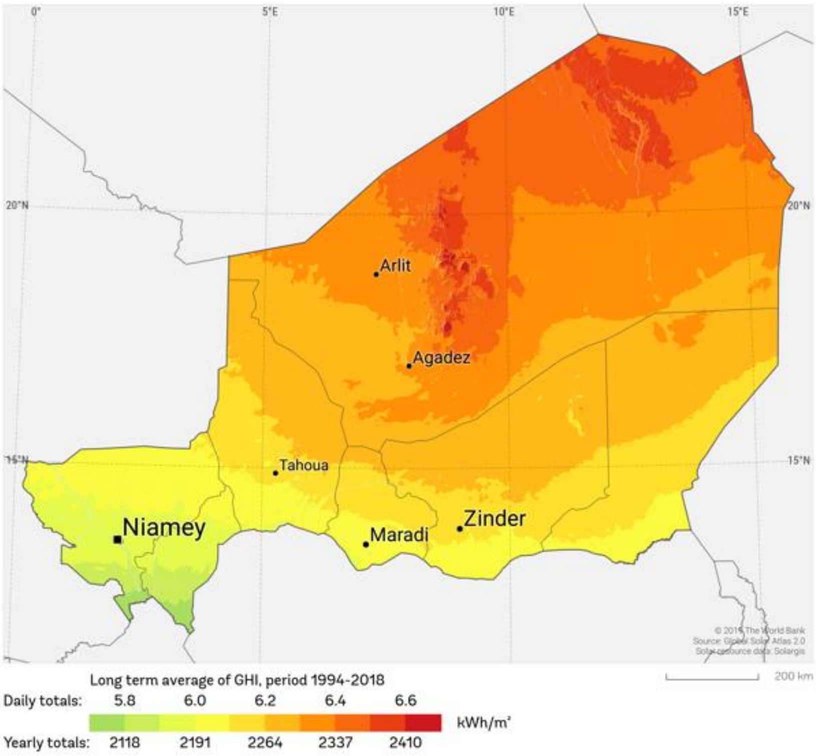

Figure 2. The global horizontal solar radiation for Niger.

The selected area for the proposed hybrid microgrid system in this study is the region of Niamey, the largest capital city and the pulsating heart of Niger. Located between latitude 13.5116° and longitude 2.1254° in the country's southwest, as shown in Figure 3, Niamey lies on the Niger River. It is the administrative, political, economic, industrial, cosmopolitan, and cultural hub of Niger, boasting modern infrastructure, and is identified as the region with the highest population, 1,500,000 [30]. Niamey experiences a semi-arid climate that is dry mainly throughout the year. There is a distinct rainy season from June to September, and the dominant season (October to May) is characterized by hot and dry weather with temperatures reaching more than 40 °C. The region is distinguished by abundant renewable energy resources, particularly solar energy, with the potential of an estimated average daily value of roughly 10.5 hours of sunshine consistently during the year [31]. The Niamey grid system is characterized by a 132 kV interconnection line extending from Birnin Kebbi (Nigeria) to Niamey (Niger), serving as the primary power supply source. This transmission line has a contractual power capacity of 120 MW; however, due to technical, contractual, or operational constraints, its actual supply is limited to an average of 50 MW. Additionally, the Niamey region's electricity demand is supplied by three local thermal power plants, Gorou Banda, Istithmar, and Niamey II, along with a local solar photovoltaic plant, with installed capacities of 80 MW, 89 MW, 22 MW, and 30 MW, respectively.

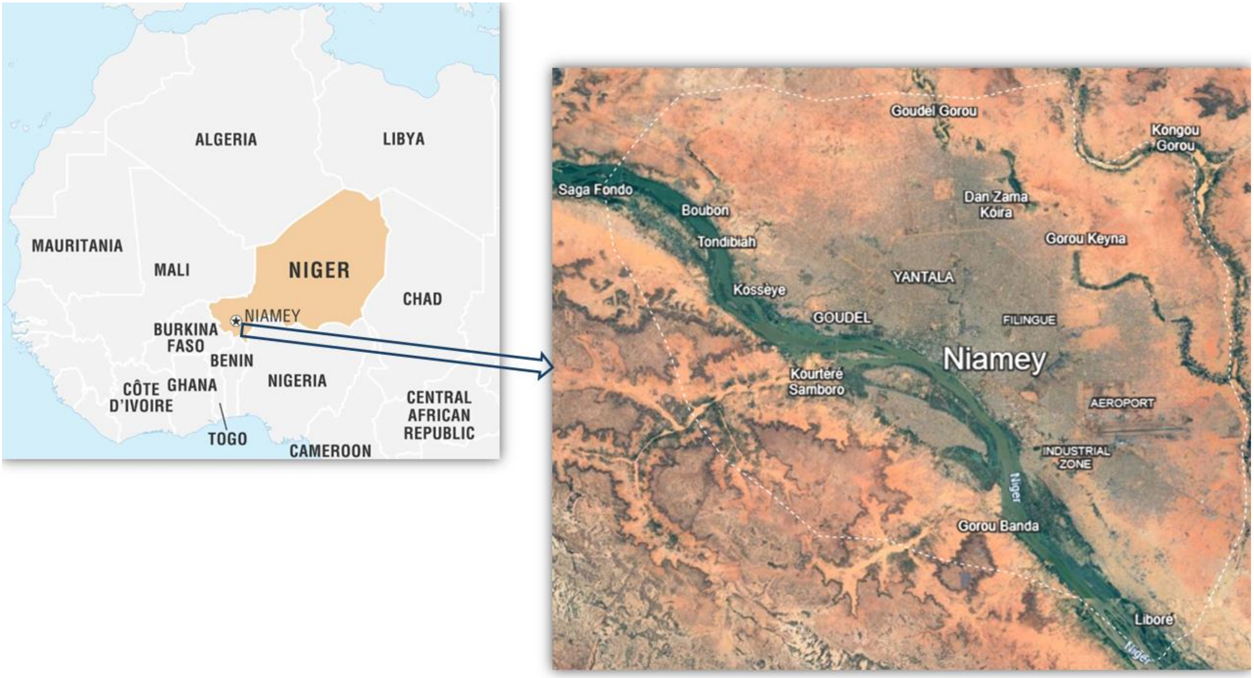

Figure 3. Google Earth map showing Niamey and its surrounding areas in Niger.

2.3. Microgrid mathematical modeling

Below are the mathematical models of photovoltaic modules, wind turbines, battery energy storage system, and hydrogen energy storage system.

2.3.1. Photovoltaic module

The sun possesses a tremendous amount of energy in the form of radiant beams that are emitted toward the Earth to fulfill the planet's energy needs. It is calculated using the following equations [32]:

$$P_{PV.th}(t) = P_{PV}\frac{I(t)}{I_{STC}}\left[1 - \beta\left(T_{AMB}(t) + \left(NOCT - T_{REF}\frac{I(t)}{I_{REF}} - T_{STC}\right)\right)\right] \tag{1}$$

$$P_{PV}(t) = \eta_{INV}(1 - f_{PV})P_{PV.th}(t) \tag{2}$$

where, $P_{PV.th}(t)$ and $P_{PV}(t)$ are the PV panel's theoretical and actual output power at time *t*.
P_{PV} is the PV panel-rated power.
$I(t)$ and $T_{AMB}(t)$ are the actual inclination solar irradiance and ambient temperature at time *t*.
I_{STC} and T_{STC} are the solar irradiance and temperature under standard test conditions.
I_{REF} and T_{REF} are the reference solar irradiance and temperature.
$NOCT$ is the nominal operating cell temperature.
β is the temperature correction coefficient.
η_{INV} is the inverter efficiency.
f_{PV} is the reduction factor in PV power production, which includes fault and maintenance, soiling and shading, and cabling loss [33].

2.3.2. Wind turbine

Wind turbines' power output depends on their technical specifications and the real-time wind speed at the hub height. The formulas is given below:

$$P_{WT.th}(t)\begin{cases} 0 \; v(t) < v_{cut-in} \\ \dfrac{v(t)^3 - v_{cut-in}^3}{v_r^3 - v_{cut-in}^3} P_r \; v_{cut-in} \le v(t) < v_r \\ P_r \; v_r \le v(t) < v_{cut-out} \\ 0 \; v(t) \ge v_{cut-out} \end{cases} \tag{3}$$

$$P_r(t) = (1 - f_w) \times P_{WT.th}(t) \tag{4}$$

where, $P_{WT.th}(t)$ and $P_r(t)$ are the theoretical and actual power output of WT at time *t*. P_r is the WT-rated power. $v(t)$ (m/s) is the wind speed at turbine hub altitude at time *t*. v_{cut-in}, $v_{cut-out}$, and v_r are WT's cut-in, cut-out, and rated wind speeds, respectively. f_W denotes the reduction factor of wind power production and encompasses various factors such as wake loss, control and turbulence, wind turbine availability, and cabling loss. The WT output power versus its speed is represented in Figure 4. The wind speed at the turbine hub altitude can be calculated using the reference speed as follows [34]:

$$v^h = v^{ref} \times \left(\frac{h}{h_{ref}}\right)^{\gamma} \tag{5}$$

where, v^{ref} is the reference speed at the height h_{ref}, and h is the turbine hub altitude. γ, a variable fall between 0.1 (representing flat terrain) and 0.25 (representing surfaces covered with forests and trees). In this paper, the area under study is considered to be flat terrain. Therefore, γ is assumed to be 0.1.

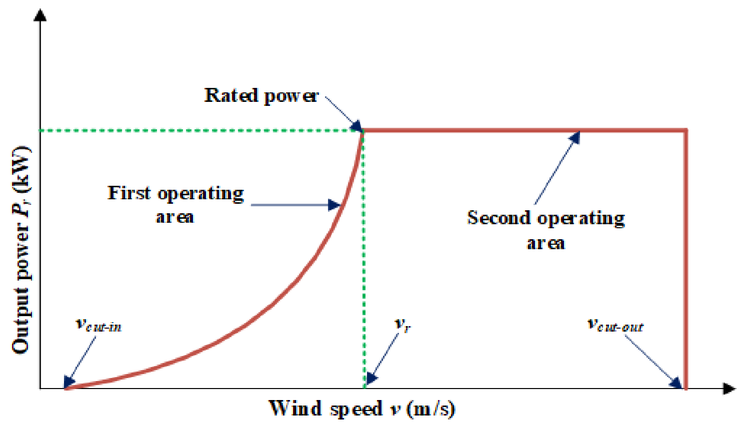

Figure 4. Power-wind speed characteristics of a standard wind turbine.

2.3.3. Battery energy storage system

Battery banks can be used as storage systems in a microgrid to balance supply and demand simultaneously. Depending on the generation and consumption of power, they can be charged or discharged, and the input power of the batteries can be either negative or positive, as shown by the equation below [35]:

$$P_B(t) = P_{PV}(t) + P_{WT}(t) - {P_{Load}(t)}/{\eta_{inv}} \quad (6)$$

where, $P_{Load}(t)$ denotes the total load demand at time t and η_{inv} the inverter efficiency.

- If $P_B = 0$, the battery bank is neither charging nor discharging. Simply, the battery bank is not in use.
- If $P_B > 0$, the battery bank is charged due to a surplus of generated power in the microgrid. In this case, Eq (7) defines the battery bank's state of charge (SOC):

$$SOC_B(t) = SOC_B(t-1) \times (1-\sigma) + \left[P_{PV}(t) + P_{WT}(t) - {P_{Load}(t)}/{\eta_{inv}}\right] \times \eta_B \quad (7)$$

- If $P_B < 0$, The battery bank is discharged due to a deficiency in the microgrid's generated power. The battery bank's SOC is defined as follows:

$$SOC_B(t) = SOC_B(t-1) \times (1-\sigma) - \left[P_{PV}(t) + P_{WT}(t) - {P_{Load}(t)}/{\eta_{inv}}\right] \times \eta_B \quad (8)$$

where, $SOC_B(t)$ and $SOC_B(t-1)$ define the battery bank SOC at the time t and $t-1$, respectively. σ is the self-discharge of the batteries and η_B is the efficiency of the batteries.

2.3.4. Hydrogen energy storage system

A hydrogen energy storage system is an advanced technology that addresses a crucial drawback of RESs (solar and wind power): Their intermittent nature. HESS can be applied to various fields, including transportation, material handling, and backup power systems. HESS consists of an electrolyzer, a hydrogen storage tank, FCs, and a local microcontroller. Figure 5 depicts a schematic diagram of a simplified HESS.

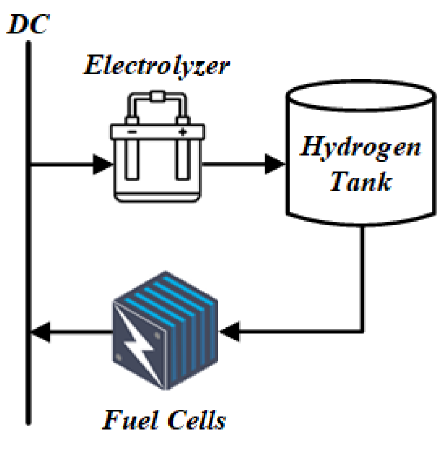

Figure 5. Simplified schematic diagram of hydrogen energy storage system.

a. Electrolyzer

The electrolyzer is a key component in hydrogen production, supplying FCs with the hydrogen necessary for electricity generation. The generated hydrogen can then be stored in a high-pressure tank until needed for various applications, including serving as a clean and efficient fuel source for FCs.

$$Electricity + H_2O = H_2 + \frac{1}{2}O_2 \tag{9}$$

The power supplied from the electrolyzer to the hydrogen storage tank can be mathematically represented as follows:

$$P_{ELE/HT} = \eta_{ELE} \times P_{Sur/ELE} \tag{10}$$

where, η_{ELE} is the electrolyzer efficiency and $P_{sur/ELE}$ denotes the surplus power supplied to the electrolyzer.

b. Hydrogen tank

Hydrogen tanks are specially designed containers that securely and efficiently store hydrogen gas, ensuring its availability for various applications, including energy generation and industrial use. Hydrogen is typically generated at a pressure of approximately 30 bar. However, when hydrogen is transferred to FCs for utilization, it is delivered at a reduced pressure of approximately 1.2 bar to ensure optimal performance and safe operation. The capacity of the hydrogen tank can be estimated using the following equation [36]:

$$V_{H_2} = \frac{m_{H_2 \times EL} \times M_{HT}}{P_{H_2} \times \rho_{H_2}} \tag{11}$$

where, $m_{H_2 \times EL}$ represents H_2 produced from the electrolyzer, M_{HT} is the margin coefficient, P_{H_2} hydrogen pressure, and ρ_{H_2} is the hydrogen density (0.089 kg/m^3).

The amount of hydrogen stored in the tank when the electrolyzer begins producing and storing hydrogen can be determined using Eq (14) [37]. When the fuel cells FCs begin consuming the stored hydrogen to compensate for power shortages, the amount of hydrogen in the storage tank can be determined using Eq (15):

$$E_{stored}(t) = E_{stored}(t-1) + \left[E_{RES}(t) - \frac{E_{Load}(t)}{\eta_{inv}}\right] \times \eta_{ELE} \tag{12}$$

$$E_{stored}(t) = E_{stored}(t-1) - \frac{\left[\frac{E_{Load}(t)}{\eta_{inv}} - E_{RES}(t)\right]}{\eta_{FCs} \times \eta_{inv}} \tag{13}$$

where, $E_{RES}(t)$ is the renewable generated power, $E_{Load}(t)$ is the load demand, and η_{inv} and η_{FCs} represent the inverter efficiency and the FCs efficiency, respectively.

c. Fuel cells

When energy demand increases or renewable sources aren't generating enough power, stored hydrogen can be used to produce electricity. In this study, proton-exchange membrane fuel cell (PEMFC) is chosen. They are widely identified as one of the common types of FCs used.

Many losses, including activation losses (V_{act}), concentration losses (V_{con}), and ohmic losses (V_{ohm}) influence the output voltage of FCs (V_{FC}). They are represented by Eqs (16), (18), (19), and (21), as follows [38]:

$$V_{FC} = E_{Nernst} - V_{act} - V_{con} - V_{ohm} \tag{14}$$

where, E_{Nernst} represents the voltage produced through a chemical reaction, as shown below.

$$E_{Nernst} = 1.229 - 8.46 \times 10^{-4}(T - 298.15) + 4.31 \times 10^{-5}T\left(ln\left(P_{H_2} \times P_{O_2}^{\frac{1}{2}}\right)\right) \tag{15}$$

where, T and P_{O_2} are the temperature and oxygen pressure, respectively.

$$V_{act} = -[\varepsilon_1 + \varepsilon_2 T + \varepsilon_3 T.ln(CO_2) + \varepsilon_4 T.ln(I_{FC})] \tag{16}$$

where, ε_1, ε_2, ε_3, and ε_4, denote the parameters of the FCs, and I_{FC} indicates the FCs current. CO_2 is the oxygen concentration defined as:

$$CO_2 = \frac{P_{O_2}}{5.08 \times 10^6 \times exp\left(\frac{-498}{T}\right)} \tag{17}$$

$$V_{con} = \frac{RT}{nF}.ln\left(1 - \frac{I_{FC}}{i_1}\right) \tag{18}$$

where, n denotes the number of electrons, R and F represent the ideal gas and Faraday constants, respectively, and i_1 is the current density limit.

$$V_{ohm} = I_{FC} \times (R_m + R_c) \tag{19}$$

where R_m and R_c are the membrane resistance and conduction resistance, respectively.

$$I_{FC} = n_{ex} \times F \times U_F \times \dot{m}_{comb} \tag{20}$$

where, n_{ex}, U_F, and $\dot{m}_{comb}$ indicate the number of electrons exchanged, the fuel utilization, and the mass flow rate ($Kg.S^{-1}$), respectively.

The output power (P_{FC}) and efficiency (η_{FC}) of the FCs can be determined using the following equations:

$$P_{FC} = V_{FC} \times I_{FC} \tag{21}$$

$$\eta_{FC} = \frac{V_{FC} \times I_{FC}}{Q_{LHV} \times U_F \times \dot{m}_{comb}} \tag{22}$$

where Q_{LHV} indicates the lower heating value ($J.Kmol^{-1}$).

3. Illustration of the proposed hybrid system

Hybrid backup systems are vital for ensuring a steady power supply in renewable-based microgrids, particularly during grid interruptions or periods of low resource availability. The proposed microgrid integrates PV and WT generation with three alternative storage configurations, each designed to enhance system stability and resilience under Niamey's climatic conditions.

3.1. Configuration 1

This system employs a BESS to manage short-term fluctuations as shown in Figure 6. The batteries charge when renewable generation exceeds demand and discharge when energy is in short supply. While this configuration offers fast response and cost efficiency, battery degradation under high temperatures limits long-term reliability.

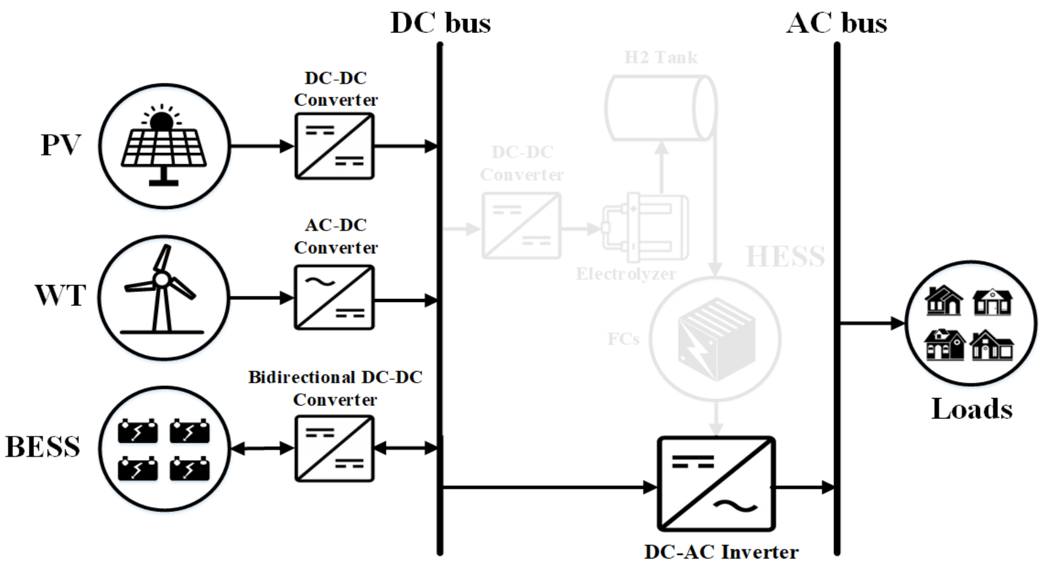

Figure 6. PV/WT/BESS system configuration.

3.2. Configuration 2

Here, surplus renewable energy is used to produce hydrogen through electrolysis. The stored hydrogen is later converted into electricity using fuel cells as shown in Figure 7. This approach supports longer-duration storage, though at a higher initial cost and lower round-trip efficiency compared to batteries.

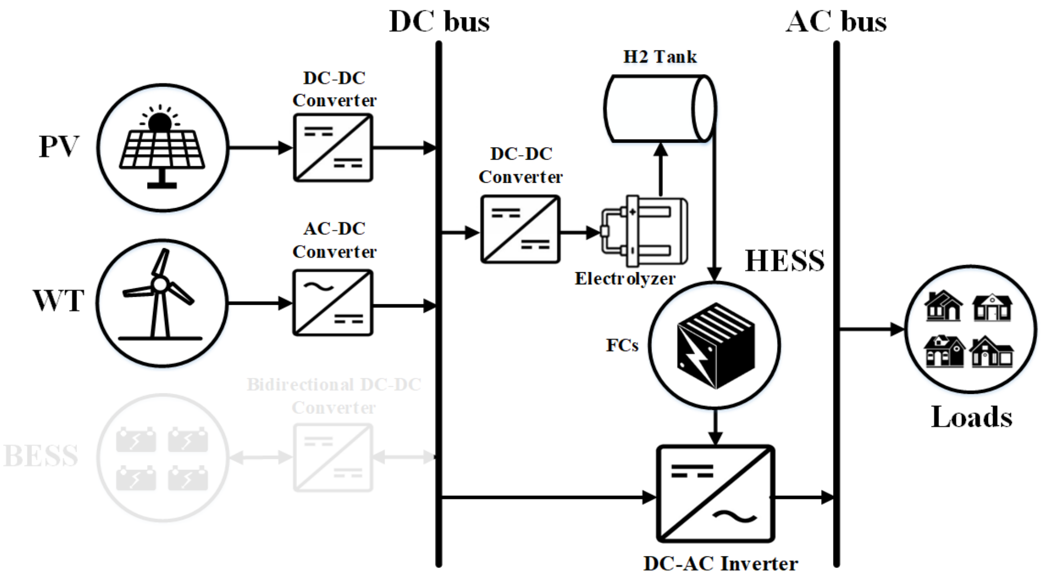

Figure 7. PV/WT/HESS system configuration.

3.3. Configuration 3

This hybrid model combines the quick-response ability of BESS with the elongate storage of HESS. Excess energy first charges the batteries, and any remaining surplus is converted into hydrogen as shown in Figure 8. The two systems operate in complementary ways, ensuring prompt and sustained energy availability. Although it requires greater investment, this configuration offers the highest level of operational flexibility and resilience.

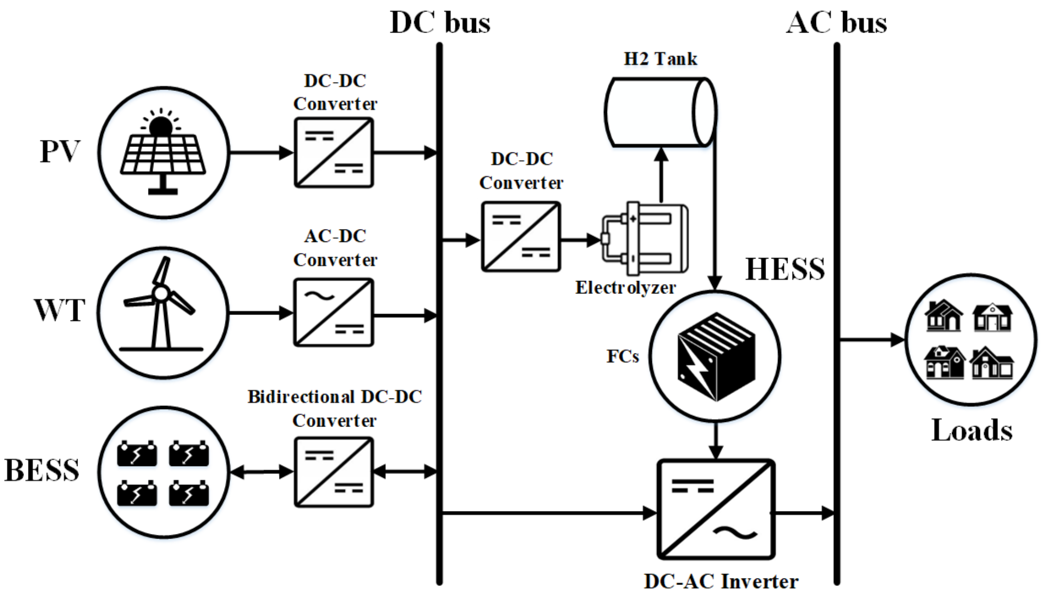

Figure 8. PV/WT/BESS/HESS system configuration.

3.4. Coordinated control of BESS and HESS

In Configuration 3, the BESS and the HESS operate under a coordinated control strategy to ensure both long-term energy stability and short-term dynamic performance of the microgrid. The integration of these two storage systems allows the microgrid to maintain energy balance, improve reliability, and mitigate fluctuations arising from intermittent renewable sources and variable load demands.

The BESS primarily addresses long-term energy management by maintaining the system's SOC within the desired operational range and optimizing the overall energy balance across the scheduling horizon. It operates on slower time scales and is responsible for storing surplus energy generated during periods of excess renewable output and supplying power during energy deficits. This strategic operation minimizes cycling stress and enhances battery life. In contrast, the HESS is designed for short-term power regulation, responding rapidly to transient power fluctuations caused by stochastic variations in renewable generation and abrupt load changes. It consists of high-power-density devices, such as supercapacitors, which complement the slower dynamics of the BESS. The HESS ensures voltage and frequency stability by absorbing or delivering power within shorter response intervals.

The coordination between BESS and HESS is achieved through a hierarchical control framework integrated within the optimization process as shown in Figure 9. The upper-level control focuses on determining the optimal energy scheduling of the BESS over the selected time horizon, ensuring efficient long-term operation and cost minimization. The lower-level control manages the instantaneous power dispatch of the HESS, ensuring rapid compensation for transient fluctuations while maintaining the microgrid's operational stability. Together, these layers establish a dynamic interaction between the two systems, enabling each to operate within its respective performance envelope.

In this study, the operational scheduling cycle is defined as daily, with hourly dispatch intervals. This temporal resolution provides an appropriate balance between computational efficiency and operational accuracy. A daily horizon is sufficiently detailed to capture short-term variations in renewable generation and load, while also enabling effective long-term energy management. Although longer scheduling cycles, such as monthly or yearly planning, can be considered for future system expansion or life-cycle cost analysis, the daily cycle adopted in this work offers the most practical compromise between precision, adaptability, and computational feasibility. The combined operation of BESS and HESS within this framework enhances the microgrid's energy resilience, improves power quality, and reduces operational cost. This coordinated strategy ensures that the BESS handles long-term energy balancing, while the HESS mitigates short-term dynamic disturbances, resulting in a reliable and efficient hybrid energy storage configuration.

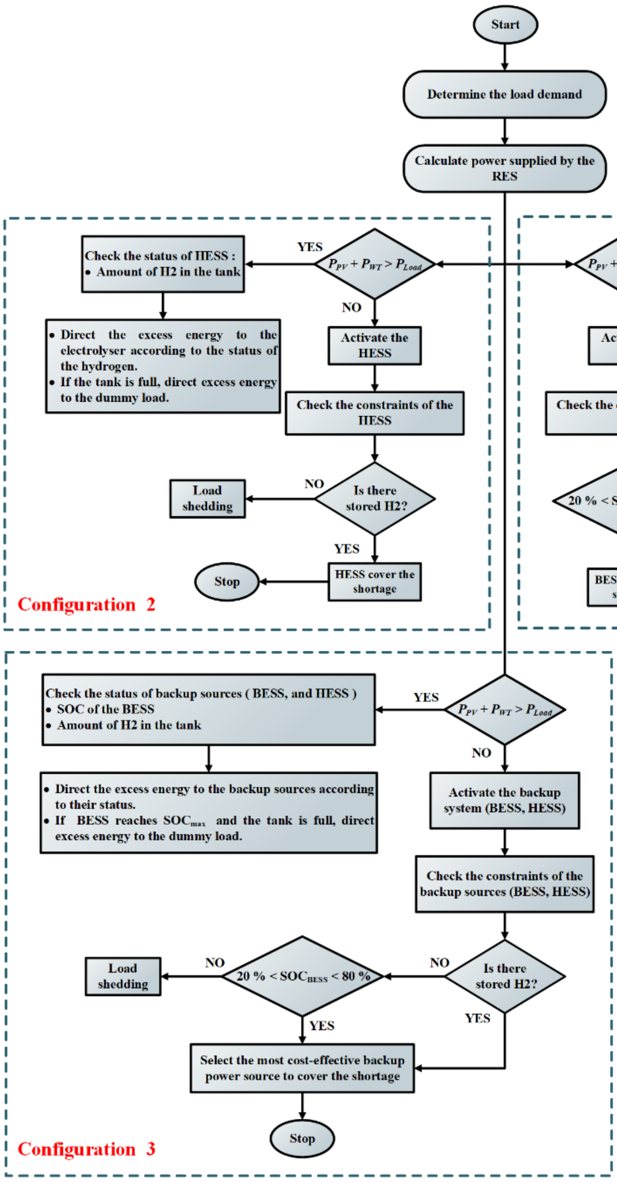

Figure 9. Flowchart of the operating mechanism of each configuration.

4. Problem formulation and proposed optimization algorithm

In this section, we describe the objective function and design constraints, and the optimization technique considered for the optimal design of the proposed microgrid system.

4.1. Objective function and design constraints

In this work, we focus on optimizing the sizing of the PV/WT/BESS/HESS to minimize the system's overall annual cost. The novelty of this work is proposing a TSA approach for determining the optimal size of the PV/WT/BESS/HESS system that minimizes the total annual cost (TAC) and covers the load demand. The general formula for the optimization problem can be expressed as follows:

$$Minimize\ f(x,y) \tag{23}$$

Subjected to constraints

$$x^{min} \leq x < x^{max} \;\&\; y^{min} \leq y < y^{max} \tag{24}$$

$$g(x,y) \geq 0 \tag{25}$$

$$h(x,y) = 0 \tag{26}$$

where $f(x,y)$ defines the objective function to be minimized, x is the vector of design variables, y is the vector of control variables, $g(x,y)$ illustrates inequality functional constraint, and $h(x,y)$ represents equality functional constraint. Our objective function denotes the hybrid system's annual total cost.

$$x = \left[N_{PV,}\, N_{WT}, N_{BESS,}\, N_{Elec,}\, N_{Tank,}\, N_{FC}, N_{Con,}\, N_{Inv}\right] \tag{27}$$

$$y = [C^C_{PV}, C^M_{PV}, C^C_{WT}, C^M_{WT}, C^C_{BESS}, C^M_{BESS}, C^C_{Elec}, C^M_{Elec}, C^C_{Tank}, C^M_{Tank}, C^C_{FC}, C^M_{FC}, C^C_{Con}, C^C_{Inv}] \tag{28}$$

where, $N_{PV,}$ N_{WT}, $N_{BESS,}$ $N_{Elec,}$ $N_{Tank,}$ N_{FC}, $N_{Con,}$ and N_{Inv} represent the number of PV panels, WT, BESS, electrolyzer, tank, Fuel Cell (FC), converter, and inverter, respectively.C^C_{PV}, C^M_{PV}, C^C_{WT}, C^M_{WT}, C^C_{BESS}, C^M_{BESS}, C^C_{Elec}, C^M_{Elec}, C^C_{Tank}, C^M_{Tank}, and C^C_{FC}, C^M_{FC}, denote the capital cost and maintenance cost of PV panels, WT, BESS, electrolyzer, tank, and FC, respectively. C^C_{Con}, and C^C_{Inv} are the cost of converter and inverter, respectively.

The objective function, which denotes the TAC of the system, can be expressed as follows:

$$f(x,y) = C^{PV}_t + C^{WT}_t + C^{BESS}_t + C^{Elec}_t + C^{Tank}_t + C^{FC}_t + C^{Con}_t + C^{Inv}_t \tag{29}$$

where, C^{PV}_t, C^{WT}_t, C^{BESS}_t, C^{Elec}_t, C^{Tank}_t, C^{FC}_t, C^{Con}_t, and C^{Inv}_t represent the total cost of the PV array system, WT, BESS, electrolyzer, tank, FC, converter, and inverter, respectively. The total cost of these components can be split into capital cost, replacement cost, and operation maintenance (O&M) costs as follows:

$$C^{PV}_t = N_{PV}\left(C^C_{PV} + \left(C^{O\&M}_{PV}\left(\frac{(1+i)^n - 1}{i(1+i)^n}\right)\right)\right) \tag{30}$$

$$C^{WT}_t = N_{WT}\left(C^C_{WT} + \left(C^{O\&M}_{WT}\left(\frac{(1+i)^n - 1}{i(1+i)^n}\right)\right)\right) \tag{31}$$

$$C^{BESS}_t = N_{BESS}\left(\begin{array}{c} C^C_{BESS} + C^R_{BESS} \displaystyle\sum_{j=1}^{j=\left(\frac{n}{n_{BESS}}-1\right)} \left(1 + \frac{1}{(1+i)^{jn_{BESS}}}\right) + \\ \left(C^{O\&M}_{BESS}\left(\frac{(1+i)^n - 1}{i(1+i)^n}\right)\right) \end{array}\right) \tag{32}$$

$$C_t^{Elec} = N_{Elec}\left(C_{Elec}^{C} + C_{Elec}^{R}\sum_{j=1}^{j=\left(\frac{n}{n_{Elec}}-1\right)}\left(1+\frac{1}{(1+i)^{jn_{ELec}}}\right)+\left(C_{Elec}^{O\&M}\left(\frac{(1+i)^n-1}{i(1+i)^n}\right)\right)\right) \quad (33)$$

$$C_t^{Tank} = N_{Tank}\left(C_{Tank}^{C} + \left(C_{Tank}^{O\&M}\left(\frac{(1+i)^n-1}{i(1+i)^n}\right)\right)\right) \quad (34)$$

$$C_t^{FC} = N_{FC}\left(C_{FC}^{C} + C_{FC}^{R}\sum_{j=1}^{j=\left(\frac{n}{n_{FC}}-1\right)}\left(1+\frac{1}{(1+i)^{jn_{FC}}}\right)+\left(C_{FC}^{O\&M}\left(\frac{(1+i)^n-1}{i(1+i)^n}\right)\right)\right) \quad (35)$$

$$C_t^{Con} = N_{Con}C_{Con}^{C} \quad (36)$$

$$C_t^{Inv} = N_{Inv}C_{Inv}^{C} \quad (37)$$

where, $C_o{}^C$, $C_o{}^R$, and $C_o{}^{O\&M}$ represent the capital cost, the replacement cost, and the operation and maintenance cost of *o* component (PV, WT, BESS, electrolyser, tank, FC, converter, or inverter). i is the interest rate, *n* is the lifetime of the system. n_{BESS}, n_{Elec}, and n_{FC} denote the lifetimes of the BESS, the electrolyzer, and the FC, respectively. Their lifetimes are assumed to be 5 years. It is observed that no replacement cost is attributed to PV/WT and H2 tanks as their lifetime is estimated to be equivalent to the system's 20-year lifespan.

The design constraints associated with the components in this study are defined as follows:

$$N_{PV}^{min} \leq N_{PV} \leq N_{PV}^{max} \quad (38)$$

$$N_{WT}^{min} \leq N_{WT} \leq N_{WT}^{max} \quad (39)$$

$$N_{BESS}^{min} \leq N_{BESS} \leq N_{BESS}^{max} \quad (40)$$

$$N_{Elec}^{min} \leq N_{Elec} \leq N_{Elec}^{max} \quad (41)$$

$$N_{Tank}^{min} \leq N_{Tank} \leq N_{Tank}^{max} \quad (42)$$

$$N_{FC}^{min} \leq N_{FC} \leq N_{FC}^{max} \quad (43)$$

$$N_{Con}^{min} \leq N_{Con} \leq N_{Con}^{max} \quad (44)$$

$$N_{Inv}^{min} \leq N_{Inv} \leq N_{Inv}^{max} \quad (45)$$

where, N_{PV}^{min}, N_{PV}^{max}, N_{WT}^{min}, N_{WT}^{max}, N_{BESS}^{min}, N_{BESS}^{max}, N_{Elec}^{min}, N_{Elec}^{max}, N_{Tank}^{min}, N_{Tank}^{max}, N_{FC}^{min}, N_{FC}^{max}, N_{Con}^{min}, N_{Con}^{max}, N_{Inv}^{min}, and N_{Inv}^{max} are the minimum and maximum values of PV modules, WT, BESS, electrolyzer, tank, FC, converter, and inverter, respectively.

The inequality functional constraint stipulates that at any given time, the sum of the power generated by the PV/WT and the power supplied by the BESS/HESS must be greater than or equal to the demand represented as follows:

$$g(x,y) = P_{PV}(t) + P_{WT}(t) + P_{BESS}(t) + P_{HESS}(t) \geq P_{Load}(t) \tag{46}$$

where, $P_{PV}(t)$, $P_{WT}(t)$, $P_{BESS}(t)$, $P_{HESS}(t)$, and $P_{Load}(t)$ denote the power output of the PV array, WT, BESS, HESS, and the load demand at time t, respectively.

The techno-economic parameters, component costs, and financial assumptions employed in the economic assessment of the proposed hybrid microgrid configurations are summarized in Table 1. The economic evaluation of the proposed hybrid microgrid configurations integrates technical and financial assumptions to ensure a realistic assessment of long-term investment feasibility. In particular, the analysis considers the influence of macroeconomic variables such as inflation, interest rate, and capital cost variability, all of which significantly affect the TAC the NPC of the system. An average inflation rate of 2.5% per year and a nominal interest rate of 6% per year are adopted, based on the most recent World Bank economic indicators for Niger (2024). The corresponding real discount rate is calculated to be approximately 3.4%.

To evaluate the robustness of the financial model, a sensitivity analysis is performed to quantify the effects of parameter fluctuations on the system's TAC. The results indicate that a ±2% variation in either the interest rate or the inflation rate can induce an approximate 5–7% change in the TAC, while a ±10% deviation in component capital costs (e.g., photovoltaic modules, wind turbines, batteries, or electrolyzers) may alter the TAC by 8–10%. These findings highlight the sensitivity of renewable energy investments to economic volatility, particularly in developing economies where access to low-interest financing and price-stabilization mechanisms is often limited.

Additional sources of uncertainty, including exchange rate fluctuations, import tariffs, and maintenance logistics, may further influence project economics, especially for hydrogen-based subsystems that rely heavily on imported technologies. To mitigate such risks, we assume stable macroeconomic conditions and gradual cost reductions consistent with international projections from the International Renewable Energy Agency (IRENA, 2023).

Overall, this analysis underscores the necessity of incorporating financial sensitivity and risk assessment into the early design stages of renewable microgrids. Continuous monitoring of macroeconomic indicators, combined with supportive policy instruments, such as tax incentives, concessional financing, and local manufacturing strategies, can enhance the long-term economic resilience and scalability of hybrid renewable systems in Niger and comparable sub-Saharan contexts.

Table 1. Summary of the techno-economic parameters, component costs, and financial assumptions employed in the economic assessment of the proposed hybrid microgrid configurations.

Component	Parameter	Value
	PV module capital cost	$7000
	PV efficiency	15%
	Temperature coefficient	0.0037
PV System [39]	Operating temperature	25 °C
	Lifetime of PV system	20 years
	PV replacement cost	$13 885/unit-year
	O&M cost	$20/unit-year

Continued on next page

Component	Parameter	Value
Wind Turbine [40]	Rated power	30 kW
	Initial cost	$58 564.79
	Replacement cost	$34 553.23
	O&M cost	3% of capital
	Lifetime	20 years
Battery Energy Storage [41]	Rated power	1 kW
	Capital cost	$500/kWh
	Replacement cost	$350/kWh
	O&M cost	$10/kWh-year
	Round-trip efficiency	90%
	Lifetime	5 years
Fuel Cell System [38,42]	Efficiency	50%
	Capital cost	$3000/unit
	Replacement cost	$2500/unit
	O&M cost	$175/unit-year
	Lifetime	5 years
Electrolyzer Unit [38,42]	Efficiency	75%
	Capital cost	$2000/unit
	Replacement cost	$1500/unit
	O&M cost	$25/unit-year
	Lifetime	20 years
Hydrogen Tank Unit [38,42]	Efficiency	95%
	Capital cost	$1300/unit
	Replacement cost	$1200/unit
	O&M cost	$15/unit-year
	Lifetime	20 years
Inverter Unit [38]	Efficiency	95%
	Capital cost	$800/unit
	Replacement cost	$750/kW
	O&M cost	$8/unit-year
	Lifespan	15 years
General Economic Parameters [13]	System lifetime	25 years
	Interest rate	6%
	Inflation rate	2.5%
	Real discount rate	3.4%
	Project lifetime	25 years

4.2. Transient search algorithm

The TSA is a metaheuristic optimization framework that draws its conceptual foundation from the transient response phenomena observed in electrical circuits, particularly first-order and second-order systems incorporating energy storage elements such as inductors and capacitors [43].

The TSA effectively integrates exploration and exploitation mechanisms, which are critical for identifying globally optimal solutions in nonlinear and multimodal optimization landscapes.

i. Theoretical foundation and inspiration

The TSA is inspired by the dynamic transient characteristics of first- and second-order electrical networks. These circuits, characterized by resistive and reactive components, exhibit responses governed by transient and steady-state behaviors. The overall system dynamics are mathematically expressed through the following governing equations:

- First-order circuits (RC or RL)

For first-order circuits, such as RC or RL configurations, the governing differential equation is formulated as:

$$\frac{d}{dt}x(t) + \frac{x(t)}{\tau} = K \tag{47}$$

The corresponding transient response can be expressed as:

$$x(t) = x(\infty) + [x(0) - x(\infty)]e^{-\frac{t}{\tau}} \tag{48}$$

- Second-order circuits (RLC)

In contrast, second-order circuits exemplified by RLC networks demonstrate more complex transient behaviors, captured by the following second-order differential equation:

$$\frac{d^2x(t)}{dt^2} + 2\alpha\frac{dx(t)}{dt} + \omega_0^2 x(t) = f(t) \tag{49}$$

The general transient response of such a system is represented as:

$$x(t) = e^{-\alpha t}[B_1\cos(2\pi f_d t) + B_2\sin(2\pi f_d t)] + x(\infty) \tag{50}$$

ii. Algorithmic structure

The TSA consists of three fundamental operational phases: Initialization, Exploration, and Exploitation. Each phase contributes to balancing stochastic global search and deterministic local refinement.

- Initialization

The algorithm begins by randomly distributing search agents within the solution domain, constrained by the lower (lb) and upper (ub) boundary limits:

$$Y = lb + rand \times (ub - lb) \tag{51}$$

- Exploration and exploitation phases

The exploration phase is primarily responsible for diversifying the search and probing unvisited regions of the solution space, thereby preventing premature convergence. Conversely, the exploitation phase inspired by the behavior of first-order circuits focuses on fine-tuning solutions around the best candidates identified so far.

A stochastic parameter, r_1, determines the balance between the two phases:

- When $r_1 < 0.5$, the algorithm engages in exploitation.
- When $r_1 \geq 0.5$, the focus shifts toward exploration.

The corresponding position-update mechanisms are defined as:

$$Y_{l+1} = Y_l^* + Y_l - C_1 Y_l^* e^{-T} (r_1 < 0.5) \tag{52}$$

$$Y_{l+1} = Y_l^* + e^{-T}[\cos(2\pi T) + \sin(2\pi T)](r_1 \geq 0.5) \tag{53}$$

These equations incorporate oscillatory dynamics, ensuring a trade-off between global diversification and localized intensification of the search process.

iii. Mathematical model for exploration-exploitation control

The transition between exploration and exploitation is mathematically modulated using the following expressions:

$$T = 2Zr_2 - Z \tag{54}$$

$$C_1 = kZr_3 + 1 \tag{55}$$

where the control parameter Z progressively decreases over iterations as:

$$Z = 2 - 2\left(\frac{l}{L_{max}}\right) \tag{56}$$

This gradual reduction enables a dynamic shift from exploration-dominant behavior at early stages to exploitation-focused refinement in later iterations, enhancing the algorithm's convergence reliability. The TSA algorithm employs these operational phases to maintain an effective equilibrium between exploration of the solution domain and exploitation for solution refinement. This strategic balance enables the algorithm to achieve high robustness and accuracy in optimization tasks. The procedural outline of the TSA algorithm is presented in Algorithm 1.

Algorithm 1 Pseudocode of the TSA Optimization Framework

Initialize the population and record the best-known positions Y_l and Y_l^*.
Compute the initial cost function for all individuals.
Repeat until the iteration count l reaches L_{max}:
    Update parameters T and C_1 using Eqs (54) and (55).
    For each search agent in Y_l:
        Update its position using Eqs (52) and (53).
    End for
    Evaluate the cost function for the updated population.
    If the new cost function yields a superior (lower) value than the current best, **update the global best** Y_l^*.
    Increment the iteration counter $l = l + 1$.
Terminate the loop upon reaching L_{max}.
Output the best solution Y_l^* obtained after all iterations.

The TSA integrates electrical circuit dynamics into an optimization framework capable of balancing exploration and exploitation with adaptive precision. By modeling the transient-steady-state interplay found in physical systems, TSA achieves enhanced global search capability and convergence stability, making it suitable for a wide range of engineering design, machine learning, and combinatorial optimization applications.

The TS algorithm employs several control parameters that govern its exploration–exploitation behavior. The adaptive and dynamic nature of these parameters ensures effective convergence while preventing premature stagnation. The key computational and control settings utilized in this study are summarized in Table 2.

Table 2. Computational and parameter settings of the TSA.

Parameter/Metric	Description	Symbol	Value/Setting
Population Size	Number of search agents used during optimization	(N_P)	30
Maximum Iterations	Total number of iterations allowe d	(L_{max})	500
Constant Parameter	Scaling factor controlling the transient search step amplitude	(k)	2
Control Variable	Adaptive parameter governing the balance between exploration and exploitation	(Z)	[0, 2]
Exploration-Exploitation Coefficient	Regulates the relative influence of global search and local refinement	(C_1)	Adaptive (Eq 55)
Transient Coefficient	Exponential decay term influencing oscillatory motion	(T)	Dynamic (Eq 54)
Random Variables	Uniformly distributed stochastic parameters used for updating positions	(r_1, r_2, r_3)	[0, 1]
Convergence Iteration	Iteration number at which the best fitness value stabilizes	I_C	410
Computational Time (s)	Total time consumed to reach convergence	T_C	12.53

4.3. Verification of the proposed optimization algorithm

The optimization problem is solved using the TSA. TSA is a metaheuristic optimization method derived from the transient response properties of electrical circuits, namely first-order and second-order circuits, including energy storage components such as inductors and capacitors [44]. The technique balances exploration and exploitation phases, which are vital in identifying the optimal solution to intricate optimization problems.

The TSA technique has undergone thorough testing and validation via benchmark functions and real-world applications to assess its efficacy and resilience in addressing optimization challenges. The primary objective of this verification method is to evaluate the algorithm's capacity to converge to optimal or near-optimal solutions in theoretical benchmark problems and practical engineering design situations. It is first evaluated for 23 benchmark functions, including single- and multi-modal ones, to verify the algorithm's generality and robustness. Single-modal functions have only one global optimum, whereas multi-modal functions have several local optima. These tests facilitate the assessment of the TSA's capacity to circumvent local minima and execute compelling exploration over the solution space. The benchmark tests evaluate several aspects of the algorithm's performance, including convergence speed, solution quality, and the balance between exploration and exploitation. The exploration phase evaluates the algorithm's capacity to discover new areas of the search space. In contrast, the exploitation phase emphasizes the capacity to fine-tune solutions and attain optimal convergence. The algorithm is run multiple times for each function to confirm that the results are consistent and reliable. The TSA's performance is assessed in comparison to the Reptile Search Algorithm (RSA) and Moth-Fame Optimization (MFO) methods. This comparison evaluates TSA's solution quality, convergence speed, and overall optimization efficiency performance over several optimization problems.

5. Results and discussions

In this case study, we examine Niamey, in the southwest of Niger, and evaluate the feasibility of implementing a microgrid. Our findings are analyzed in detail in the following subsections:

5.1. Case study

Designing microgrid systems that integrate RESs can provide a pathway to meeting the energy demands of cities and their communities and, to some extent, reaching energy independence, economic stability, and environmental sustainability [45,46]. However, these systems cannot fulfill the energy demand needs due to RESs and electricity demand fluctuations. Integrating storage systems has proven an effective solution with considerable potential to mitigate these fluctuation problems. This approach entails storing excess energy generated by RESs in ESSs, which can later be used during periods of reduced energy production to meet electricity demand. Integrating storage systems can improve RESs' economic and technical viability. Niamey, the capital city of Niger, in the southwestern region of the country, is chosen as the focus area for this study. The climatic conditions in this location promote the generation of a substantial amount of energy from renewable sources (PV and WT). The daily solar irradiance and temperature in Niamey are depicted in Figures 10 and 11, respectively. Niamey has a promising solar irradiance throughout the day (6 am–6 pm), with a significant increase between early morning and afternoon, peaking at 1 pm (918.26 W/m^2), as shown in Figure 10. The region is also characterized by high temperatures all day round with average daily temperature up to 35 ºC, as indicated in Figure 11. Likewise, the wind speed is favorable for electrical power generation. Wind speed is high during the morning and night, as shown in Figure 12. The proposed approach is assessed on a particular day in May. The day selected for the simulation corresponds to a typical day in May, which represents the period of highest temperature and peak load demand in Niamey. This month was intentionally chosen to evaluate system performance under the most critical operating conditions in terms of solar irradiance, temperature, and load variation. Using a single representative day is a standard approach in microgrid optimization studies, as it allows for thorough analysis of the system's dynamic behavior while keeping computational complexity manageable. The same optimization framework can be extended to seasonal studies in future work to confirm the system's performance throughout the year.

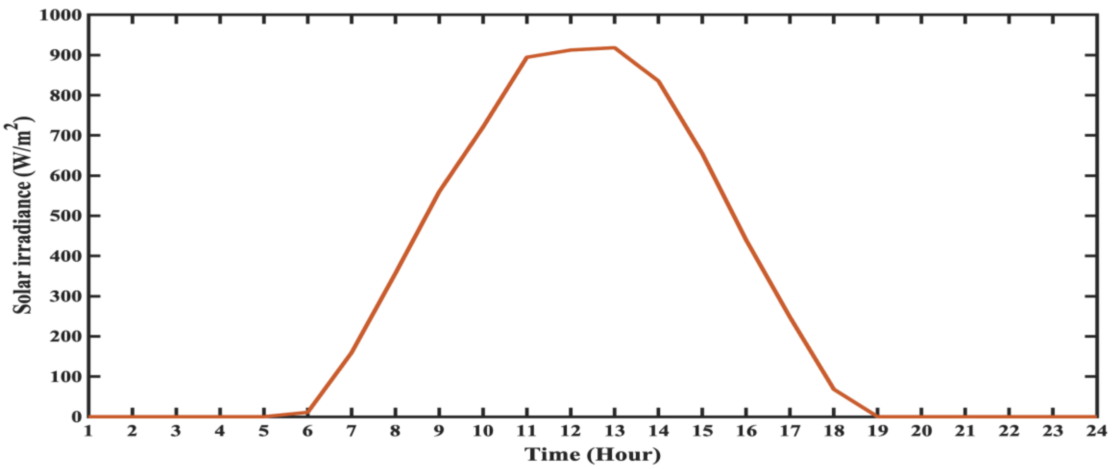

Figure 10. Daily solar irradiance of Niamey.

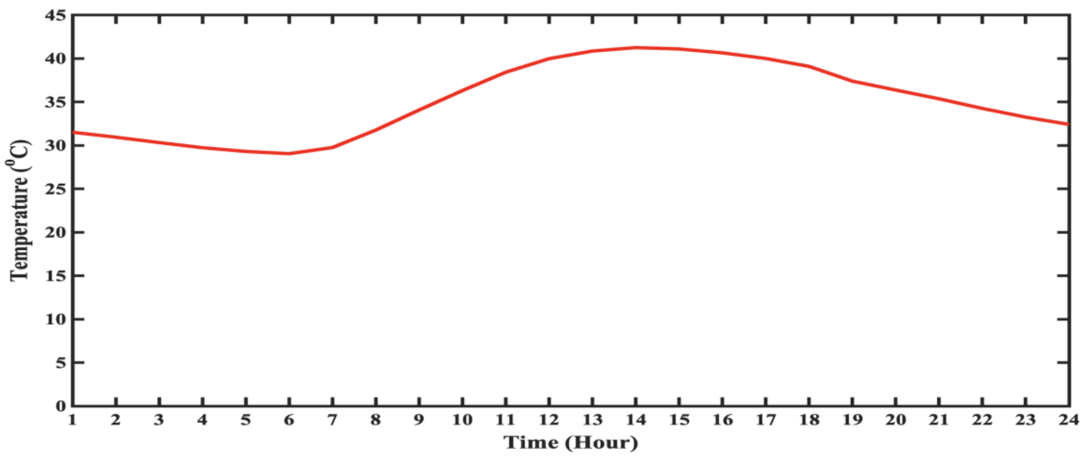

Figure 11. Daily temperature of Niamey.

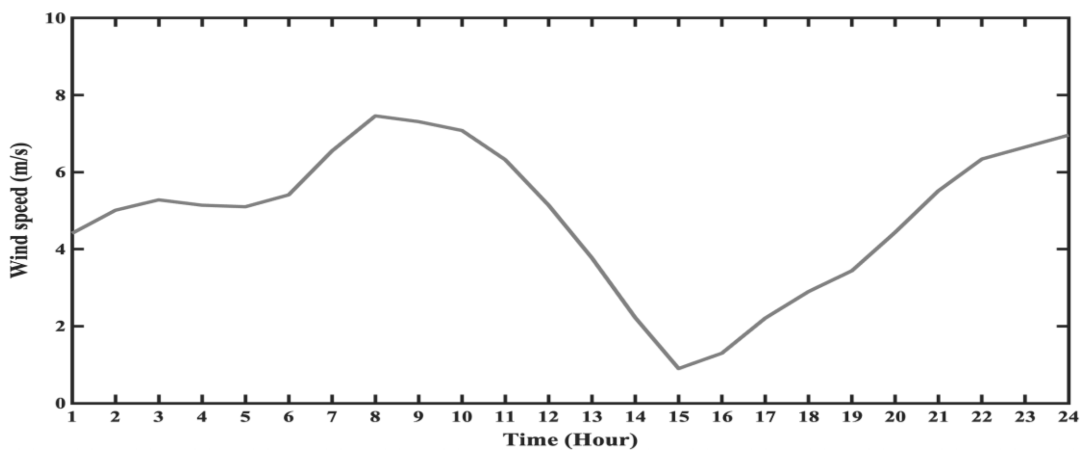

Figure 12. Daily wind speed of Niamey.

5.2. Configuration results

5.2.1. Configuration 1

This scheme analyzes power contributions from the system's components load, PV/WT/BESS, over 24 hours. Throughout the day, the load demand demonstrated consistent fluctuations, with the highest demand occurring between 12 pm and 6 pm, and a slight increase observed during the nighttime hours (10 pm to 1 am). The peak demand reached 182.82 MW at 5 pm and 177.78 MW at 12 am, as illustrated in Figure 13. On the other hand, the load demand dropped between 6 am and 10 am, with the lowest value being 115.09 MW, recorded at 8 am. The PV panels started generating power at 6 am and ceased at 6 pm, as shown in Figure 13. During these daylight hours, their generation is characterized by a distinct peak power output during noontime when the sun is at its zenith, resulting in maximum solar irradiance. This peak value is approximately 162.645 MW at 1 pm, as depicted by Figure 13. Further, wind power, serving as the second leading source, shows a more variable trend. Wind power generation is directly controlled by wind speed. The power generated reached maximum values of 175.045 MW and 147.633 MW at 8 am and 12 am, respectively, as depicted in Figure 13. The period 7 am to 10 am marked relatively low demand, and wind power is at its maximum values, as shown in Figure 13. During this low-demand period, the excess power generated by WT is directed to charge the BESS, securing its availability for usage during peak loads or scarcity of RESs. The BESS's contribution displays a coordination role, alternating between positive values (discharging) to meet the load demand when generation is inadequate and negative values (charging) during periods of oversupply. Figure 13 shows the maximum BESS discharging power values during the early evening and late night, reaching up to 182.09 MW at 6 pm when the demand tops the RESs generated power. This strategic discharge pattern ensures a reliable power supply, effectively meeting energy demands despite variations in RESs availability. From early morning to afternoon, when solar irradiance gradually increases, PV and wind power are generated to satisfy energy needs. During the same period, excess power is generated and is then used to charge the BESS for late use.

Figure 14 describes the hourly variation in BESS over 24 hours. The storage levels begin at an increased value, around 2000 MWh, during the initial hours of the day and decrease toward the end of the day. The energy storage peaks around midday (12 pm–1 pm). This is likely correlated with RESs generation, especially PV array systems, where irradiance is maximum. A gradual drop follows due to higher discharge or lower input from RESs during the early evening and midnight.

The annual total cost of configuration 1, which integrates PV panels, WT, and the BESS, amounts to $18,605,642,775.90. This total cost is calculated over the project lifespan of 25 years, ensuring a comprehensive evaluation of the long-term financial implications. This configuration is the most cost-effective among the three, primarily due to the lower capital investment required for BESS than hydrogen-based storage. Batteries offer an efficient and relatively affordable means of energy storage, making them an attractive option for microgrid implementations. However, the reliability of this system is limited by the characteristics of battery storage technology.

While BESS can quickly respond to fluctuations in renewable energy generation and provide immediate backup power, its limited storage capacity, and relatively short cycle life, typically between five and ten years, pose reliability concerns. Frequent charge and discharge cycles lead to battery degradation, requiring periodic replacements contributing to long-term operational costs. Given that the system’s operational timeframe spans 25 years, multiple battery replacements are expected, influencing overall cost-effectiveness and maintenance planning. Furthermore, during extended periods of low renewable generation, such as prolonged cloudy days or low wind speeds, the battery storage may not be enough to meet the demand, potentially resulting in power shortages.

From a reliability perspective, this configuration is best suited for short-term energy fluctuations rather than prolonged outages. It is highly dependent on consistent renewable generation, and any prolonged energy supply gap may require additional backup solutions, such as grid integration or diesel generators. Although cost-effective, its reliance on BESS alone makes it less resilient in handling prolonged renewable intermittency, which could impact critical loads in Niamey, particularly during adverse weather conditions.

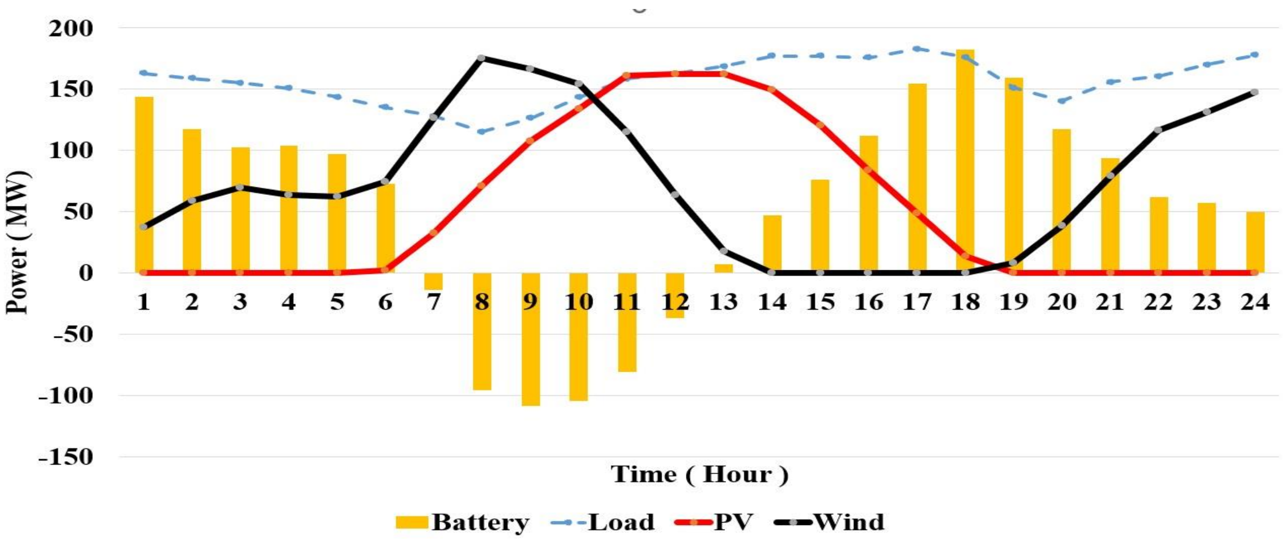

Figure 13. The hourly contribution from main sources and BESS in meeting the electricity demand in configuration 1.

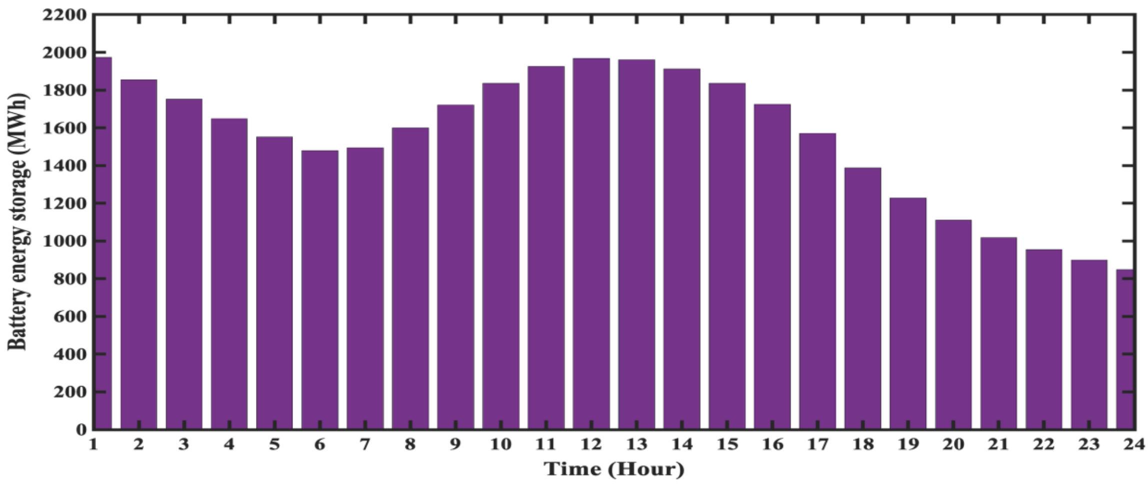

Figure 14. The hourly battery energy storage in configuration 1.

5.2.2. Configuration 2

HESS is incorporated in addition to the primary sources (PV and WT) in this configuration. HESS integration provides an effective solution for storing, conserving, and supplying energy. This technology holds considerable promise for energy storage, ensuring a reliable energy supply and improving the microgrid's overall stability. As noted earlier, the daily load in Niamey exhibits a fluctuating pattern throughout the day, as depicted in Figure 15. The contribution of HESS to the power supply during this period demonstrates its potential for providing a reliable and consistent energy source, enhancing the system's overall stability and reliability. HESS's power output decreases from 7 pm to midnight and late at night, around 2 am. Moreover, HESS does not contribute in the early morning and midday hours. This is due to enough generation from RESs, which satisfies the power demand with surplus energy produced. The surplus energy was utilized for hydrogen production, which is an efficient method for storing and using excess renewable energy. By converting surplus energy into hydrogen, the system can store it and use it in fuel cells FCs when required. This hydrogen-generating technology offers enhanced flexibility in energy source management. Figure 16 reveals the hourly variation in the tank energy storage over a day. The storage level begins at an increased value of around 2700 MWh during the early hours, particularly at 1 am. This indicates that the tank had accumulated energy from the system during nighttime hours when the demand was low. However, this storage gradually decreases from late night to early morning hours as energy is discharged to meet the demand. Around midday, the tank storage reaches high levels; relatively steady levels are observed between 11 am and 2 pm. This phenomenon is associated with simultaneous high RESs generation and decreased reliance on stored energy. Following this, there is a constant decline from 3 pm until the end of the day. This drop matches the increasing load demand and reduced RESs inputs, resulting in a more significant dependence on tank storage.

Configuration 2's annual total cost, which incorporates a HESS instead of BESS, is \$26,299,141,964.71, significantly more expensive than configuration 1. This total cost is calculated for the 25-year project lifespan, ensuring a comprehensive financial assessment of long-term hydrogen-based storage deployment. The cost increase is primarily attributed to the high capital expenses associated with hydrogen infrastructure, including electrolyzers, hydrogen storage tanks, and fuel cells. While this configuration demands a more significant financial investment, it offers a higher level of reliability and long-term energy security.

Unlike BESS, hydrogen storage does not degrade over time. It can store excess renewable energy for longer durations, making it a more resilient solution for mitigating prolonged periods of low renewable generation. Over the 25-year project period, this long-term storage capability significantly enhances system stability, reducing the need for frequent replacements and mitigating the financial impact of battery degradation seen in BESS-based configurations. This is particularly important in Niamey, where energy supply interruptions due to climatic variability or geopolitical issues, such as disruptions in power imports from Nigeria, pose significant risks. By converting surplus renewable energy into hydrogen and storing it for later use, HESS ensures a more stable and continuous power supply, reducing the likelihood of outages during prolonged renewable intermittency.

However, HESS is less efficient than BESS in immediate response scenarios. The conversion losses in electrolysis and fuel cell operation result in lower overall energy efficiency than direct battery storage. Although hydrogen storage provides long-term reliability, the efficiency trade-offs must be carefully considered over the 25-year project horizon, particularly regarding energy conversion losses and operational management. Hydrogen infrastructure requires specialized handling, safety considerations, and a well-managed control system to ensure optimal operation. Despite these challenges, hydrogen's long-term reliability and extended storage capacity make this configuration better suited for large-scale energy resilience and future-proofing the microgrid against disruptions.

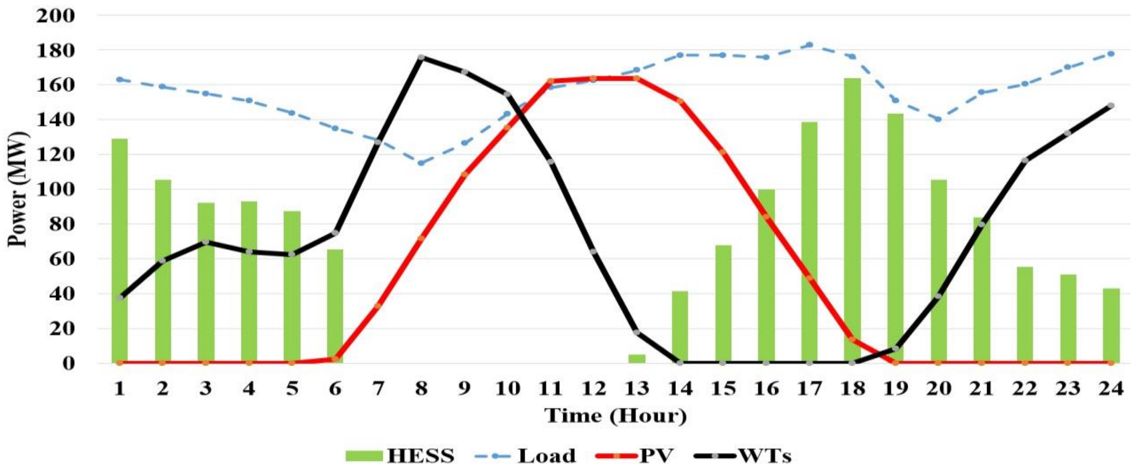

Figure 15. The hourly contribution from main sources and HESS in meeting the electricity demand in configuration 2.

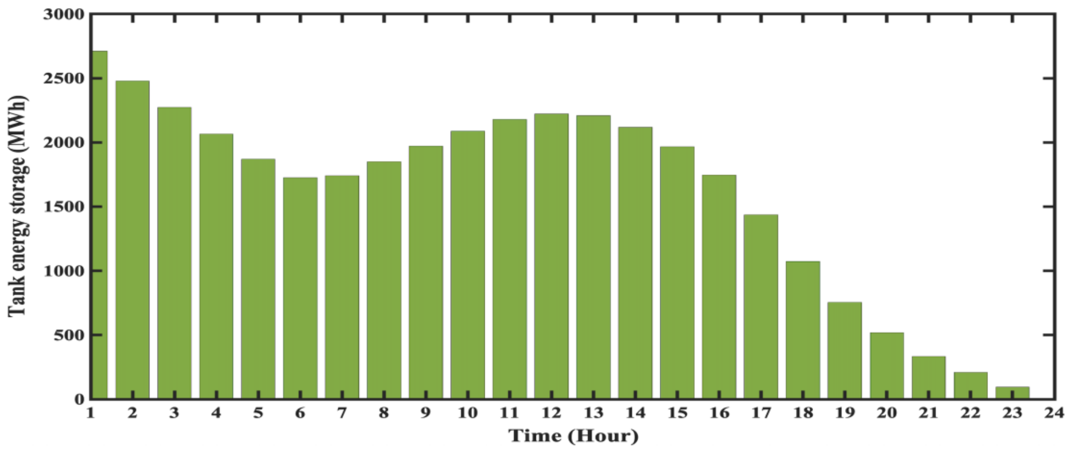

Figure 16. The hourly tank energy storage in configuration 2.

5.2.3. Configuration 3

This configuration utilizes backup sources BESS and HESS alongside the primary sources (PV and WT) to fulfill the load demand throughout the day. During the morning hours, the load shows relatively low values, PV presents high values, and WT shows high and then low values toward midday. This causes the generation to be higher than the needs, as shown in Figure 17. During this period, surplus energy is produced and used to charge the BESS, ensuring it is available for future use. From 1 pm to 7 pm, there is no power generated by the WT, and the output from the PV system gradually decreases, resulting in an energy shortage. As a result, the HESS is activated to provide the additional energy required to cover the deficit. During the early night hours, WT and high contribution of BESS are used to satisfy the demands. The BESS is crucial and contributes considerably to meeting the demand. Its maximum contribution is around 161.726 MW at 7 pm. From late night to early morning, the load slightly decreases and cannot be met by the WT power, as depicted in Figure 17. To clear this deficit, HESS contributes fully to meeting the electrical load demand. Its highest contribution (1–6 am) is approximately 138.531 MW at 1 am. The dynamics of the BESS and HESS highlight their essential role in addressing energy shortages at different times of the day, ensuring a stable and consistent power supply while efficiently optimizing the use of available energy sources. Figure 18 depicts the hourly variation in BESS over 24 hours. The storage levels are relatively steady during the early hours and begin to increase gradually from 8 am. At noon, the stored energy peaks at 1028.235 MWh, which is stable until 5 pm. The increased value observed from 8 am to 12 pm and the stable value between 12 pm and 5 pm indicate active charging, driven by surplus energy from PV and WT. A Steady decline is followed in the evening and night. This is due to the reserve depletion of the BESS that began discharging to support the load demand as RESs generation declined, particularly PV.

Figure 19 shows the energy storage in the tank system over a day. During the initial hours, the tank storage levels start at a high value of 2242.152 MWh at 1 am, implying prior charging correlated to low demand and wind power availability. A gradual decline follows until noon when the storage level stabilizes due to concurrent power input from PV and WT. Further, the tank storage was considerably depleted in the evening, reaching minimal levels as the day ended.

Configuration 3, which integrates BESS and HESS alongside PV and wind energy, incurs the highest annual total cost at $27,128,616,936.07. This cost reflects the investment required for short-term and long-term energy storage solutions over the operational lifespan of the system. This hybrid approach combines the advantages of short-term and long-term energy storage, significantly improving system resilience and reliability. While the cost is substantial due to the dual storage infrastructure, this configuration offers the highest level of energy security and flexibility among the three options.

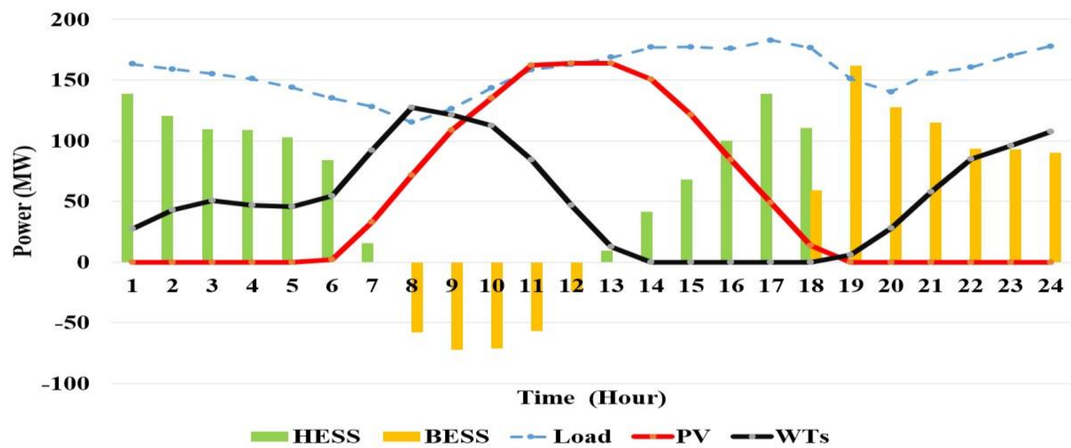

Figure 17. The hourly contribution from main and backup (BESS and HESS) sources in meeting the electricity demand in configuration 3.

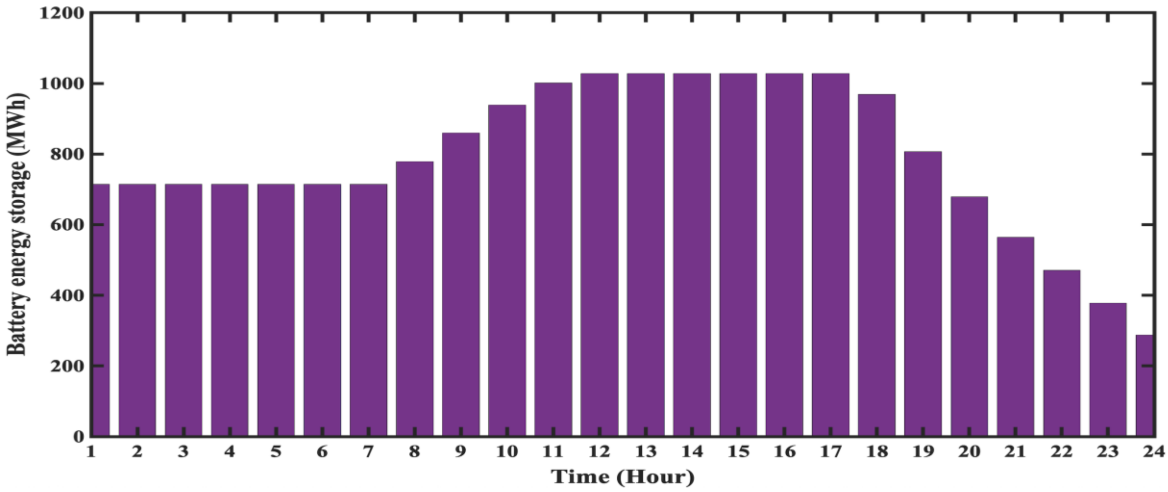

Figure 18. The hourly battery energy storage in configuration 3.

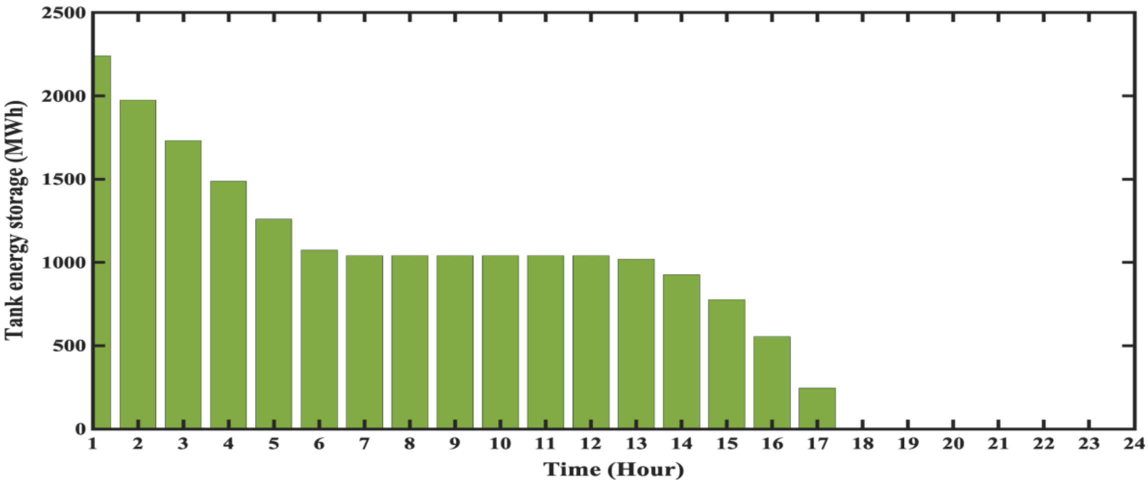

Figure 19. The hourly tank energy storage in configuration 3.

By leveraging BESS for short-term, high-efficiency storage, and HESS for long-duration energy storage, this system can effectively handle immediate fluctuations in renewable generation and extended power outages throughout the 25-year period. BESS ensures rapid response to load variations, providing instant power balancing, while HESS acts as a long-term energy reserve, supplying electricity when renewable sources are insufficient for prolonged periods. This dual-storage strategy mitigates energy shortages more effectively than standalone BESS or HESS configurations, ensuring stable power supply even in scenarios of extended renewable intermittency. This combination minimizes the risks of energy shortages, particularly during extreme weather events, geopolitical energy supply disruptions, or grid failures.

From a reliability standpoint, this configuration is the most robust and resilient option for the 25-year operational period, offering an optimal balance between short-term and long-term energy security. It ensures that energy demand is met under all circumstances, making it ideal for critical infrastructure, hospitals, and industrial facilities that require uninterrupted power supply. However, the high financial cost associated with maintaining both storage systems over 25 years presents a challenge, requiring careful economic planning, potential government subsidies, or financing mechanisms to make the solution more viable for large-scale deployment.

5.3. System scalability and future adaptability

Scalability and adaptability are critical considerations for the long-term success of microgrid systems in Niamey, Niger, where energy demand is rising due to urban population growth, economic expansion, and increasing electricity needs for industries and essential services. A well-designed microgrid should be capable of expanding its capacity to meet these increasing demands while integrating emerging renewable energy technologies to enhance efficiency and sustainability. In this section, we evaluate the scalability of the three proposed configurations and their adaptability to future energy advancements in Niamey.

Each configuration has different scalability capabilities depending on the storage system efficiency, availability of renewable resources, and feasibility of infrastructure expansion in Niamey. The reliance on BESS in configuration 1 as the primary storage technology limits scalability due to the high cost, short cycle life, and sensitivity of batteries to Niamey's high temperatures. The extreme heat could accelerate battery degradation, increasing the frequency of replacements and raising long-term operational costs. Expanding the system to accommodate higher energy demand would require significant battery capacity additions, increasing capital and maintenance costs. Additionally, land availability for large-scale battery storage may be challenging in urban Niamey. In configuration 2, hydrogen storage provides better scalability than BESS due to its longer storage duration and higher energy density. In Niamey, where seasonal variations in solar and wind energy exist, hydrogen storage can help mitigate long-term energy shortages, making it more adaptable to fluctuating demand. Moreover, hydrogen can be stored indefinitely, unlike batteries that degrade over time. However, the high initial investment cost of electrolyzers, hydrogen storage tanks, and fuel cells, combined with limited hydrogen infrastructure and water resource constraints for electrolysis, poses a challenge for immediate large-scale expansion. In configuration 3, the dual-storage approach enhances scalability by balancing short-term and long-term energy storage solutions. The combination of BESS for rapid response and HESS for prolonged energy storage enables the system to support higher load demands, particularly for critical loads such as hospitals, industrial zones, and public services in Niamey. However, managing two storage systems increases system complexity and operational costs, requiring advanced energy management strategies and government incentives to optimize scalability and economic feasibility.

Since Niamey and surrounding regions experience frequent power outages, voltage instability, and reliance on electricity imports, microgrid systems should be designed for islanded operation, meaning they must function independently without grid support. By integrating solar, wind, and energy storage, the microgrid can provide continuous electricity supply even during periods of low renewable energy generation. Configuration 3, which combines BESS and HESS, offers the best reliability for islanded operation by ensuring both short-term and long-term energy availability. Since Niamey's power grid is often unstable, a standalone microgrid system ensures that critical facilities such as hospitals, water supply systems, and communication networks remain operational even during nationwide blackouts. Transitioning to an independent, renewable-based microgrid system reduces reliance on imported electricity from Nigeria, strengthening energy security and economic stability in Niger. As energy storage and renewable energy technologies evolve, future improvements will enhance the efficiency, scalability, and cost-effectiveness of microgrid configurations in Niamey.

Microgrid configurations' scalability and future adaptability in Niamey depend on technological advancements, economic incentives, and strategic energy policies. Configuration 1 faces scalability challenges due to battery limitations. In contrast, configuration 2 offers long-term resilience through hydrogen storage. Configuration 3 provides the most balanced and resilient solution for ensuring energy security and sustainability in off-grid and islanded applications. Future developments in battery technology, hydrogen production efficiency, and smart energy integration will be crucial in determining the feasibility of large-scale microgrid deployment in Niamey.

5.4. Quantitative environmental impact and CO_2 reduction analysis

To complement the techno-economic evaluation, a detailed quantitative assessment of the environmental performance of the three optimized hybrid microgrid configurations is conducted. This analysis focuses on estimating the annual and life-cycle carbon dioxide (CO_2) emission reductions resulting from the displacement of fossil-based grid electricity by renewable generation. The baseline emission factor for the Nigerian-sourced grid electricity imported to Niger is assumed to be 0.68 kg CO_2 per kWh, based on the most recent data from the International Energy Agency (IEA, 2023). The annual CO_2 mitigation for each configuration is computed using the optimized renewable energy generation results obtained through the TSA, considering a 25-year project lifetime. Table 3 presents a comparative summary of the estimated annual and cumulative CO_2 reductions for the three configurations. All systems achieve significant emission mitigation, demonstrating the potential of hybrid renewable microgrids to reduce greenhouse gas (GHG) emissions while enhancing local energy security in Niger.

The results reveal that all configurations substantially contribute to carbon emission reduction, with total life-cycle savings ranging from approximately 71,575 to 73,950 tons of CO_2 over the 25-year period. This highlights the strong environmental potential of renewable microgrids as a decarbonization strategy for developing regions with fossil-dependent power imports.

The PV/WT/BESS configuration achieves an annual CO_2 reduction of 2,863 tons, corresponding to 71,575 tons over its lifetime. This configuration benefits from high battery round-trip efficiency (~90%) and stable short-term energy storage, enabling consistent renewable energy utilization. However, its overall CO_2 reduction potential is slightly constrained by limited storage duration, which results in occasional renewable energy curtailment during extended periods of low solar and wind output. Consequently, although the configuration is the most economically favorable, it provides moderate environmental benefits relative to the hybrid alternatives.

The PV/WT/HESS configuration achieves a slightly higher reduction of 2,924 tons of CO_2 per year, totaling 73,100 tons over the system lifetime. The integration of HESS enables long-term energy retention through electrolyzer–fuel cell conversion, facilitating more stable power supply during prolonged renewable intermittency. This reduces curtailment losses and enhances renewable utilization. Nonetheless, the system's overall emission advantage is partially offset by conversion inefficiencies inherent in the hydrogen cycle, where round-trip efficiencies typically range from 35% to 45%. Despite these losses, the configuration performs better environmentally than the battery-only system, primarily due to its extended storage capability and improved renewable integration.

The PV/WT/BESS/HESS hybrid configuration exhibits the most favorable environmental performance, with an annual CO_2 reduction of 2,958 tons and a cumulative saving of approximately 73,950 tons over the 25-year period. The combined use of short-term (BESS) and long-term (HESS) storage technologies ensures higher renewable energy capture and minimal curtailment, resulting in near-complete utilization of available solar and wind resources. This synergy between the two storage mechanisms enhances operational flexibility, reliability, and sustainability. The configuration, therefore, represents the optimal trade-off between economic feasibility and environmental benefit, delivering the highest emission reduction while maintaining system stability and resilience.

In summary, the comparative analysis demonstrates that integrating complementary storage technologies substantially enhances the environmental performance of renewable microgrids. Although the PV/WT/BESS system remains the most cost-efficient, the hybrid PV/WT/BESS/HESS configuration offers the greatest sustainability advantage due to its superior capacity for renewable energy utilization and emission avoidance. Over its life cycle, the hybrid system is estimated to achieve approximately 3% greater CO_2 reduction than the battery-only configuration.

These findings confirm that the deployment of hybrid storage systems can play a decisive role in achieving low-carbon energy transitions in regions such as Niger. The results align with the country's Nationally Determined Contributions (NDCs) under the Paris Agreement and contribute directly to Sustainable Development Goal (SDG) 7 on affordable and clean energy, and SDG 13 on climate action. Therefore, the proposed hybrid configuration not only strengthens energy reliability and economic resilience but also provides a measurable contribution to climate change mitigation.

Table 3. Estimated CO_2 emission reduction and life-cycle environmental benefits of the three configurations.

Configuration	Renewable share (%)	Annual generation (MWh)	CO_2 reduction (tons/year)	Life-cycle CO_2 reduction (tons/25 years)
PV + WT + BESS	100	4,210	2,863	71,575
PV + WT + HESS	100	4,300	2,924	73,100
PV + WT + BESS + HESS	100	4,350	2,958	73,950

5.5. Operational challenges and mitigation strategies

The successful implementation of a renewable-based microgrid in Niamey, Niger, faces several technical, financial, and environmental challenges. Given the hot climate, limited grid infrastructure, and economic constraints, addressing these challenges with appropriate mitigation strategies is essential to ensure reliable and sustainable energy access. In this section, we highlight the key operational challenges associated with microgrid deployment in Niamey and outlines strategies to overcome them. One of the significant technical challenges is the intermittency of RESs. Niamey benefits from high solar irradiance throughout the year, but wind speeds fluctuate seasonally, leading to variability in power generation. Dust storms and the Harmattan season can also reduce solar panel efficiency, further impacting energy reliability. To mitigate these issues, an optimized hybrid storage system combining BESS and HESS (Configuration 3) can ensure continuous electricity supply by storing excess renewable energy and dispatching it when needed. Additionally, integrating advanced forecasting systems and AI-driven energy management can improve power dispatch based on weather predictions and demand patterns. Overcapacity in solar and wind generation can also help compensate for days with lower renewable energy availability.

Another significant concern is the impact of high temperatures on battery storage. Niamey's extreme heat accelerates battery degradation, reducing the lifespan of BESS and increasing replacement costs. This issue can be mitigated by selecting temperature-resistant battery technologies, such as lithium-titanate (LTO) or sodium-ion batteries with higher thermal stability. Implementing passive cooling solutions, such as shaded enclosures, reflective coatings, and underground storage units, can minimize battery overheating. Reducing the dependence on BESS by incorporating HESS for long-duration storage can also improve system reliability and extend battery lifespan. Hydrogen storage, despite its advantages, presents its own set of challenges. The cost of electrolyzers and fuel cells remains high, and the process requires a substantial amount of water. The potential water consumption for electrolysis must be carefully managed to avoid conflicts with the drinking water supply. Low-water-consumption electrolysis technologies and wastewater recycling for hydrogen production should be explored to address this issue. Solid-state hydrogen storage or high-pressure composite tanks can also help minimize hydrogen losses and improve storage efficiency.

Deploying renewable-based microgrids in Niamey presents several operational challenges, including renewable intermittency, battery degradation, hydrogen storage limitations, high financial costs, and environmental constraints. However, these challenges can be effectively mitigated by implementing advanced energy management solutions, improved cooling techniques, financial incentives, and community engagement strategies. With strong policy support and investment in sustainable energy solutions, microgrid deployment can be vital in enhancing energy security, reducing emissions, and supporting economic development in Niamey, Niger.

6. Conclusions

Niamey has faced persistent challenges in ensuring a stable, reliable, and sustainable electricity supply over the long term due to its heavy dependence on imported energy and the intermittent nature of renewable sources. The city's electricity infrastructure struggles with frequent power shortages and fluctuations, making it challenging to meet the growing demand from households, businesses, and critical facilities such as hospitals and schools. Given Niamey's high solar potential and moderate wind availability, integrating renewable energy microgrids has become a viable solution to address energy shortages while reducing reliance on imports. However, the efficiency and reliability of renewable systems depend greatly on the choice of energy storage technologies and their ability to balance supply and demand over the 25-year project lifespan.

To tackle these issues, we investigate three renewable-based microgrid configurations, each incorporating different energy storage solutions to enhance energy security and system resilience. The proposed configurations include PV/WT/BESS, PV/WT/HESS, and PV/WT/BESS/HESS, each presenting unique trade-offs between cost, reliability, and scalability. To determine the optimal system design, a robust and efficient TSA is employed. This metaheuristic optimization technique effectively balanced cost minimization, energy supply stability, and storage performance by considering solar and wind energy availability variability over the 25-year period. The objective function is formulated to achieve the lowest total cost over the full project duration, while ensuring an optimal mix of generation capacity, storage efficiency, and economic feasibility. The optimization results and cost analysis lead to the following conclusions:

1. Configuration 1 (PV/WT/BESS) proved to be the most economical system over the 25-year project period, with a total cost of $18.6 billion. The system relies on BESS for energy storage, which

offers an effective short-term solution but presents long-term reliability concerns due to battery degradation and high replacement costs. Over time, BESS's limited cycle life and reduced efficiency in high-temperature conditions contribute to increased operational expenses and storage limitations, making this configuration less ideal for long-term deployment without periodic battery replacements.

2. Configuration 2 (PV/WT/HESS) introduced hydrogen energy storage (HESS), enhancing long-duration energy storage and reducing power shortages over extended periods of low solar or wind generation. The use of hydrogen as an alternative storage medium increased the system's ability to maintain energy supply stability. However, this improvement came at a significantly higher cost, raising the total 25-year project cost to $26.3 billion, representing a 41.3% increase compared to configuration 1. The main reason for this cost rise is the substantial capital investment required for electrolyzers, hydrogen storage tanks, and fuel cells, all of which add financial complexity to system implementation and long-term operation.
3. Configuration 3 (PV/WT/BESS/HESS) incorporated BESS and HESS, creating a hybrid storage system that balances short-term and long-term energy needs. By leveraging the rapid response of BESS and the extended storage capacity of HESS, this configuration provided the most resilient and flexible energy storage solution over the 25-year period. The total cost reached $27.1 billion, reflecting a 3.2% increase over configuration 2 and a 45.8% increase compared to configuration 1. Despite the higher investment, this hybrid system minimized renewable energy curtailment, improved system reliability, and ensured optimal power availability, making it the most technically robust solution for Niamey in the long term.
4. Configuration 1 was the most cost-effective option in terms of upfront investment, but its limited storage capacity made it vulnerable to energy deficits, particularly during extended low-sunlight or low-wind periods over the 25-year lifespan. Although configuration 2 mitigated this issue by integrating hydrogen storage, it significantly increased overall system costs due to high capital expenditures. In contrast, configuration 3 ensured long-term reliability while maintaining only a marginal cost increase compared to configuration 2, making it the most balanced trade-off between cost and performance.
5. The high capital cost of HESS remains a significant financial barrier to large-scale deployment, particularly in developing energy markets such as Niamey. However, technological advancements in electrolyzer efficiency, reductions in fuel cell costs, and government incentives could significantly lower the cost of hydrogen-based storage systems over the 25-year operational period. If hydrogen production costs decline, hybrid storage solutions like configuration 3 could become more economically feasible for long-term implementation in Niamey.

This study demonstrated that hybrid energy storage solutions provide superior energy reliability. Still, their higher upfront costs must be addressed through cost-reduction strategies, improved energy management solutions, and targeted policy interventions. In the future, researchers should focus on the economic feasibility of hydrogen energy storage, including the potential for cost reductions through mass production, efficiency improvements in electrolyzers, and financial incentives for hydrogen adoption. Additionally, integrating intelligent energy management systems with AI-based forecasting and dynamic energy dispatch strategies could further enhance system efficiency and cost-effectiveness. In addition, future research will also include a comprehensive comparative investigation between the proposed TSA and other well-established optimization techniques. In future work, we will focus on implementing each method under identical operating conditions, datasets, and techno-economic parameters to ensure a fair evaluation. Our objective will be to quantitatively assess performance differences in terms of convergence speed, solution accuracy, computational efficiency, and robustness, thereby providing a clearer understanding of the relative advantages of the TSA approach

Use of AI tools declaration

The authors declare they have not used Artificial Intelligence (AI) tools in the creation of this article.

Conflict of interest

The authors declare that they have no known competing financial interests or personal relationships that could have appeared to influence the work reported in this paper.

Prof. Tomonobu Senjyu is an editorial board member for AIMS Energy and was not involved in the editorial review or the decision to publish this article. All authors declare that there are no competing interests.

Author contributions

Issoufou Tahirou Halidou: Conceptualization, Methodology, Formal analysis, Investigation, Writing—original draft. M. H. Elkholy: Conceptualization—review and editing. Akie Uehara: Supervision—review and editing. Fathia Jombi Kheir: Writing—review and editing. Mitsunaga Kinjo: Supervision—review and editing. Tomonobu Senjyu: Conceptualization, Resources, Supervision, Administration. M. Talaat: Supervision—review and editing. Abdoulkader Moussa Siddo: Writing—review and editing. Taghreed Said: Conceptualization—review and editing.

References

1. Abbass K, Qasim MZ, Song H, et al. (2022) A review of the global climate change impacts, adaptation, and sustainable mitigation measures. *Environ Sci Pollut Res* 29: 42539–42559. https://doi.org/10.1007/s11356-022-19718-6
2. Chen XH, Tee K, Elnahass M, et al. (2023) Assessing the environmental impacts of renewable energy sources: A case study on air pollution and carbon emissions in China. *J Environ Manag* 345: 118525. https://doi.org/10.1016/j.jenvman.2023.118525
3. Amin MA, Farhad Z (2024) Power transmission in Afghanistan: Challenges, opportunities and proposals. *AIMS Energy* 12: 840–871. https://doi.org/10.3934/energy.2024040
4. Alblawi A, Said T, Talaat M, et al. (2022) PV solar power forecasting based on hybrid MFFNN-ALO. *2022 13th International Conference on Electrical Engineering (ICEENG)*, 52–56. https://doi.org/10.1109/ICEENG49683.2022.9782040
5. Priyanka S (2022) Eco-Friendly energy resources. *Scieng* 4: 87–98.
6. Mahmood D, Javaid N, Ahmed G, et al. (2021) A review on optimization strategies integrating renewable energy sources focusing uncertainty factor–Paving path to eco-friendly smart cities. *Sustainable Comput: Inf Syst* 30: 100559. https://doi.org/10.1016/j.suscom.2021.100559

7. Bertaglia T, Costa CM, Lanceros-Méndez S, et al. (2024) Eco-friendly, sustainable, and safe energy storage: A nature-inspired materials paradigm shift. *Mater Adv* 5: 7534–7547. https://doi.org/10.1039/D4MA00363B
8. Chen R, Song D, Liao L, et al. (2025) Feedback correction scheduling strategy for electric vehicles based on multi-regional agent master-slave and evolutionary hybrid game. *Energy* 319: 134984. https://doi.org/10.1016/j.energy.2025.134984.
9. Talaat M, Mohamed AR, Sedhom BE, et al. (2024) Monolithic design of self-adaptive CMOS converter and robust event-triggered consensus control for integration of multi-renewable energy sources with battery storage system. *J Energy Storage* 88: 111498. https://doi.org/10.1016/j.est.2024.111498.
10. Elkholy MH, Yona A, Ueda S, et al. (2024) Experimental investigation of ai-enhanced FPGA-based optimal management and control of an isolated microgrid. *IEEE Trans Transp Electrification* 10: 3670–3679. https://doi.org/10.1109/TTE.2023.3315729
11. Zohuri B, Zohuri B (2018) Hybrid renewable energy systems. *Hybrid Energy Syst: Driving Reliab Renewable Sources Energy Storage*, 1–38. https://doi.org/10.1007/978-3-319-70721-1_1
12. Tahirou Halidou I, Or Rashid Howlader H, Gamil MM, et al. (2023) Optimal power scheduling and techno-economic analysis of a residential microgrid for a remotely located area: a case study for the sahara desert of Niger. *Energies* 16: 3471. https://doi.org/10.3390/en16083471
13. Ahmed S, Huang Y, Tayyab Q, et al. (2024) Identification of power grids low-frequency oscillations through a combined MEEMD-Prony method. *Energy Rep* 11: 4245–4253. https://doi.org/10.1016/j.egyr.2024.04.015
14. Song D, Yousaf A, Noor J, et al. (2025) ANN-Based model predictive control for hybrid energy storage systems in DC microgrid. *Prot Control Mod Power Syst* 10: 1–15. https://doi.org/10.23919/PCMP.2024.000074
15. Ahmed S, Rashid H, Qadir Z, et al. (2025) Deep learning-based recognition and classification of soiled photovoltaic modules using HALCON software for solar cleaning robots. *Sensors* 25: 1295. https://doi.org/10.3390/s25051295
16. Shang C, Srinivasan D, Reindl T (2016) Generation-scheduling-coupled battery sizing of stand-alone hybrid power systems. *Energy* 114: 671–682. https://doi.org/10.1016/j.energy.2016.07.123
17. Fodhil F, Hamidat A, Nadjemi O (2019) Potential, optimization and sensitivity analysis of photovoltaic-diesel-battery hybrid energy system for rural electrification in Algeria. *Energy* 169: 613–624. https://doi.org/10.1016/j.energy.2018.12.049
18. Zhang Y, Lundblad A, Campana PE, et al. (2016) Employing battery storage to increase photovoltaic self-sufficiency in a residential building of Sweden. *Energy Procedia* 88: 455–461. https://doi.org/10.1016/j.egypro.2016.06.025
19. Amrollahi MH, Bathaee SMT (2017) Techno-economic optimization of hybrid photovoltaic/wind generation together with energy storage system in a stand-alone micro-grid subjected to demand response. *Appl Energy* 202: 66–77. https://doi.org/10.1016/j.apenergy.2017.05.116
20. Ren H, Wu Q, Gao W, et al. (2016) Optimal operation of a grid-connected hybrid PV/fuel cell/battery energy system for residential applications. *Energy* 113: 702–712. https://doi.org/10.1016/j.energy.2016.07.091

21. Kiptoo MK, Lotfy ME, Adewuyi OB, et al. (2020) Integrated approach for optimal techno-economic planning for high renewable energy-based isolated microgrid considering cost of energy storage and demand response strategies. *Energy Convers Manage* 215: 112917. https://doi.org/10.1016/j.enconman.2020.112917
22. Shabani M, Dahlquist E, Wallin F, et al. (2020) Techno-economic comparison of optimal design of renewable-battery storage and renewable micro pumped hydro storage power supply systems: A case study in Sweden. *Appl Energy* 279: 115830. https://doi.org/10.1016/j.apenergy.2020.115830
23. Esparcia Jr EA, Castro MT, Odulio CMF, et al. (2022) A stochastic techno-economic comparison of generation-integrated long duration flywheel, lithium-ion battery, and lead-acid battery energy storage technologies for isolated microgrid applications. *J Energy Storage* 52: 104681. https://doi.org/10.1016/j.est.2022.104681
24. Eteiba M, Barakat S, Samy M, et al. (2018) Optimization of an off-grid PV/Biomass hybrid system with different battery technologies. *Sustainable Cities Soc* 40: 713–727. https://doi.org/10.1016/j.scs.2018.01.012
25. Kumar P, Pal N, Sharma H (2021) Techno-economic analysis of solar photo-voltaic/diesel generator hybrid system using different energy storage technologies for isolated islands of India. *J Energy Storage* 41: 102965. https://doi.org/10.1016/j.est.2021.102965
26. Liu T, Yang J, Yang Z, et al. (2022) Techno-economic feasibility of solar power plants considering PV/CSP with electrical/thermal energy storage system. *Energy Convers Manage* 255: 115308. https://doi.org/10.1016/j.enconman.2022.115308
27. Xu F, Liu J, Lin S, et al. (2018) A multi-objective optimization model of hybrid energy storage system for non-grid-connected wind power: A case study in China. *Energy* 163: 585–603. https://doi.org/10.1016/j.energy.2018.08.152
28. Niger's uranium remains focus of international interest. *Nucl Eng Int*. Available from: https://www.neimagazine.com/news/nigers-uranium-remains-focus-of-international-interest/?cf-view&cf-click&cf-minimized&cf-view.
29. Macrotrends. Niamey, Niger Metro Area Population 1950–2024. Available from: https://www.macrotrends.net/global-metrics/cities/21972/niamey/population#:~:text=The%20current%20metro%20area%20population,a%203.59%25%20increase%20from%202021.
30. Climate. Niamey Climate (Niger). Available from: https://en.climate-data.org/africa/niger/niamey/niamey-497/.
31. He Y, Guo S, Zhou J, et al. (2021) The many-objective optimal design of renewable energy cogeneration system. *Energy* 234: 121244. https://doi.org/10.1016/j.energy.2021.121244
32. Guo S, He Y, Pei H, et al. (2020) The multi-objective capacity optimization of wind-photovoltaic-thermal energy storage hybrid power system with electric heater. *Sol Energy* 195: 138–149. https://doi.org/10.1016/j.solener.2019.11.063
33. Kaabeche A, Ibtiouen R (2014) Techno-economic optimization of hybrid photovoltaic/wind/diesel/battery generation in a stand-alone power system. *Sol Energy* 103: 171–182. https://doi.org/10.1016/j.solener.2014.02.017
34. Abd El-Sattar H, Kamel S, Sultan HM, et al. (2022) Optimal design of photovoltaic, biomass, fuel cell, hydrogen tank units and electrolyzer hybrid system for a remote area in Egypt. *Energy Rep* 8: 9506–9527. https://doi.org/10.1016/j.egyr.2022.07.060

35. Smaoui M, Abdelkafi A, Krichen L (2015) Optimal sizing of stand-alone photovoltaic/wind/hydrogen hybrid system supplying a desalination unit. *Sol Energy* 120: 263–276. https://doi.org/10.1016/j.solener.2015.07.032.
36. Maleki A, Pourfayaz F (2015) Sizing of stand-alone photovoltaic/wind/diesel system with battery and fuel cell storage devices by harmony search algorithm. *J Energy Storage* 2: 30–42. https://doi.org/10.1016/j.est.2015.05.006
37. Diab AAZ, Sultan HM, Mohamed IS, et al. (2019) Application of different optimization algorithms for optimal sizing of PV/Wind/Diesel/Battery storage stand-alone hybrid microgrid. *IEEE Access* 7: 119223–119245. https://doi.org/10.1109/ACCESS.2019.2936656
38. Sultan HM, Menesy AS, Kamel S, et al. (2021) An improved artificial ecosystem optimization algorithm for optimal configuration of a hybrid PV/WT/FC energy system. *Alexandria Eng J* 60: 1001–1025. https://doi.org/10.1016/j.aej.2020.10.027
39. Sultan HM, Kuznetsov ON, Menesy AS, et al. (2020) Optimal configuration of a grid-connected hybrid PV/Wind/Hydro-Pumped storage power system based on a novel optimization algorithm. *2020 International Youth Conference on Radio Electronics, Electrical and Power Engineering (REEPE)*, 1–7. https://doi.org/10.1109/REEPE49198.2020.9059189
40. Pai L, Senjyu T, Elkholy MH (2024) Integrated home energy management with hybrid backup storage and vehicle-to-home systems for enhanced resilience, efficiency, and energy independence in green buildings. *Appl Sci* 14: 7747. https://doi.org/10.3390/app14177747
41. Elkholy MH, Senjyu T, Gamil MM, et al. (2024) Implementation of a multistage predictive energy management strategy considering electric vehicles using a novel hybrid optimization technique. *J Cleaner Prod* 476: 143765. https://doi.org/10.1016/j.jclepro.2024.143765
42. Fathy A (2016) A reliable methodology based on mine blast optimization algorithm for optimal sizing of hybrid PV-wind-FC system for remote area in Egypt. *Renewable Energy* 95: 367–380. https://doi.org/10.1016/j.renene.2016.04.030
43. Qais MH, Hasanien HM, Alghuwainem S (2020) Transient search optimization: A new meta-heuristic optimization algorithm. *Appl Intell* 50: 3926–3941. https://doi.org/10.1007/s10489-020-01727-y
44. Al-Ghussain L, Ahmad AD, Abubaker AM, et al. (2021) An integrated photovoltaic/wind/biomass and hybrid energy storage systems towards 100% renewable energy microgrids in university campuses. *Sustainable Energy Technol Assess* 46: 101273. https://doi.org/10.1016/j.seta.2021.101273
45. Mostafaeipour A, Rezayat H, Rezaei M (2020) A thorough investigation of solar-powered hydrogen potential and accurate location planning for big cities: A case study. *Int J Hydrogen Energy* 45: 31599–31611. https://doi.org/10.1016/j.ijhydene.2020.08.211
46. Gamil MM, Ueda S, Nakadomari A, et al. (2022) Optimal multi-objective power scheduling of a residential microgrid considering renewable sources and demand response technique. *Sustainability* 14: 13709. Available from: https://www.mdpi.com/2071-1050/14/21/13709.